



CREaTE

Canterbury Research and Theses Environment

Canterbury Christ Church University's repository of research outputs

<http://create.canterbury.ac.uk>

Please cite this publication as follows:

Caputo, L., Witzel, H. R., Kolovos, P., Cheedipudi, S., Looso, M., Mylona, A., van Ijcken, W., Evans, S. M., Braun, T., Soler, E., Grosveld, F. and Dobreva, G. (2015) The Isl1/Ldb1 complex orchestrates heart-specific chromatin organization and transcriptional regulation. *Cell Stem Cell*, 17 (3). pp. 287-299. ISSN 1934-5909.

Link to official URL (if available):

<http://dx.doi.org/10.1016/j.stem.2015.08.007>

This version is made available in accordance with publishers' policies. All material made available by CReaTE is protected by intellectual property law, including copyright law. Any use made of the contents should comply with the relevant law.

Contact: create.library@canterbury.ac.uk



**The Isl1/Ldb1 complex orchestrates
heart-specific chromatin organization and transcriptional regulation**

Luca Caputo¹, Hagen R. Witzel¹, Petros Kolovos², Sirisha Cheedipudi¹, Mario Looso¹, Athina Mylona², Wilfred F.J. van Ijcken³, Karl-Ludwig Laugwitz⁴, Sylvia M. Evans⁵, Thomas Braun¹, Eric Soler^{2,6}, Frank Grosveld² and Gergana Dobрева^{1,7*}

¹Max Planck Institute for Heart and Lung Research, Bad Nauheim, Germany

²Department of Cell Biology, Erasmus Medical Center, Rotterdam, The Netherlands

³Center for Biomics, Erasmus Medical Center, Rotterdam, The Netherlands

⁴I. Medizinische Klinik und Poliklinik, Klinikum rechts der Isar der Technischen Universität München, Ismaninger Strasse 22, Munich, Germany

⁵Department of Medicine, Skaggs School of Pharmacy, University of California, San Diego, California, USA

⁶Laboratory of Molecular Hematopoiesis, CEA/DSV/iRCM/LHM, INSERM UMR967, Fontenay-aux-Roses, France

⁷Medical Faculty, University of Frankfurt, 60590 Frankfurt am Main, Germany

*Correspondence: Gergana.Dobрева@mpi-bn.mpg.de

Tel: +49-06032-705-259

Fax: +49-06032-705-211

Keywords: Isl1, Ldb1, Mef2c, Hand2, cardiac progenitors, cardiomyocyte differentiation, second heart field, long-range interactions, AHF enhancer, genome organization

Running title: Role of Ldb1 in cardiogenesis

SUMMARY

Cardiac stem/progenitor cells hold great potential for regenerative therapies, however, the mechanisms regulating their expansion and differentiation remain insufficiently defined. Here we show that the multi-adaptor protein Ldb1 is a central regulator of cardiac progenitor cell differentiation and second heart field (SHF) development. Mechanistically, we demonstrate that Ldb1 binds to the key regulator of SHF progenitors Isl1 and protects it from proteasomal degradation. Furthermore, the Isl1/Ldb1 complex promotes long-range promoter-enhancer interactions at the loci of the core cardiac transcription factors *Mef2c* and *Hand2*. Chromosome conformation capture followed by sequencing identified surprisingly specific, Ldb1-mediated interactions of the Isl1/Ldb1 responsive *Mef2c* anterior heart field enhancer with genes which play key roles in cardiac progenitor cell function and cardiovascular development. Importantly, the expression of these genes was downregulated upon Ldb1 depletion and Isl1/Ldb1 haploinsufficiency. In conclusion, the Isl1/Ldb1 complex orchestrates a network for heart-specific transcriptional regulation and coordination in three-dimensional space during cardiogenesis.

INTRODUCTION

Heart failure is the leading cause of morbidity and mortality worldwide. Due to the limited regenerative capacity of the human heart, cardiomyocytes lost during heart injury are substituted by a non-contractile fibrotic scar tissue, resulting in decreased cardiac function and ultimately heart failure. A number of cardiac regenerative strategies have been proposed of which stem/progenitor cells hold great promise for heart repair (Aguirre et al., 2013; Hansson et al., 2009; Laflamme and Murry, 2011). Knowledge accumulated from developmental studies have significantly improved the methods for *in vitro* cardiac differentiation from embryonic stem (ES) cells and studies utilizing ES differentiation have brought further insights in the regulatory networks integrating multiple transcription factors and signaling molecules, which strictly control the distinct steps of cardiogenesis. However, the current limitations for the use of stem/progenitor cells in regenerative medicine, e.g. linked to their expansion, differentiation efficiency and functional integration, call for a more complete understanding of the mechanisms driving cardiovascular lineage commitment, expansion and differentiation.

During embryogenesis the heart is generated by a common progenitor at gastrulation that segregates into two distinct populations, termed first and second heart fields. The first heart field (FHF), fuses at the midline and differentiates into the myocardium of the heart tube. After the initial heart tube formation, the heart tube grows by addition of Isl1-positive second heart field (SHF) progenitor cells to its anterior and venous poles (Cai et al., 2003; Evans et al., 2010; Vincent and Buckingham, 2010). Studies in different model systems revealed the crucial function of the LIM-homeodomain transcription factor Isl1 in heart morphogenesis (Cai et al., 2003; de Pater et al., 2009; Witzel et al., 2012). Isl1-deficient mouse embryos lack the right ventricle and the outflow tract, both structures derived from the SHF, as Isl1 is required for the proliferation, survival, and migration of these cells into the forming heart (Cai et al., 2003). Importantly, the Isl1-positive cardiovascular progenitors are multipotent and can differentiate into all three cardiovascular lineages: cardiomyocytes, smooth muscle cells and endothelial cells (Moretti et

al., 2006). Moreover, *Isl1* is required for the differentiation of these cells into the cardiomyocyte and smooth muscle lineage (Kwon et al., 2009), but the mechanisms underlying its function are poorly understood.

The acquisition of cellular identity involves genome reorganization and a coordinated series of large-scale transcriptional changes (Dixon et al., 2015; Dixon et al., 2012; Gorkin et al., 2014; Peric-Hupkes et al., 2010). Using chromosome conformation capture (3C) assays and 3C-based technologies (de Wit and de Laat, 2012; Dekker et al., 2002) recent studies have suggested that CTCF together with Cohesin might be involved in general formation of chromatin structures by promoting constitutive long-range DNA interactions, whereas specific transcription factors, their co-factors together with CTCF, Cohesin and the Mediator complex might be involved in controlling locus-specific looping interactions and lineage-specific transcription (Kagey et al., 2010; Phillips-Cremins et al., 2013; Shen et al., 2012). In ES cells for example the binding of the key pluripotency transcription factors Oct4, Sox2, and Nanog was shown to be a key determinant of genome organization, as regions with a high density of binding sites for these factors tend to colocalize in nuclear space (de Wit et al., 2013; Denholtz et al., 2013). Another example for a cofactor involved in promoting locus-specific and cell type-specific interactions is Ldb1 (Deng et al., 2012; Morcillo et al., 1997; Soler et al., 2010; Song et al., 2007). Ldb1 directly binds to LIM domain- and Otx proteins and is found in large complexes with bHLH and GATA transcription factors (Bach et al., 1997; Jurata et al., 1998; Meier et al., 2006; Tripic et al., 2009). By bringing together distinct transcription factors and their coregulators, associated with different transcriptional control elements, Ldb1 facilitates long range promoter-enhancer interactions and regulates cell-type specific expression patterns (Deng et al., 2012; Morcillo et al., 1997; Soler et al., 2010; Song et al., 2007).

Here we show that Ldb1 is a multifunctional regulator of SHF development and cardiac differentiation. We show that the importance of Ldb1 for SHF development is two-fold. On the one hand, Ldb1 binds to *Isl1* and protects it from proteasomal degradation, as a consequence of

which *Ldb1*-deficiency leads to an almost complete loss of *Isl1*⁺ cardiovascular progenitor cells. On the other hand, the *Isl1/Ldb1* complex promotes long-range promoter enhancer interactions at the loci of the key developmental regulators of cardiogenesis *Mef2c* and *Hand2*. Using 3C-seq we identified specific *Ldb1*-mediated interactions of the *Mef2c* AHF enhancer with genes which play key roles in cardiovascular development as well as cell fate commitment. Moreover, *Ldb1*-deficient cells and *Isl1/Ldb1* haplodeficient embryos, which show various cardiac anomalies, show a dramatically decreased expression of genes associated with the AHF enhancer and overexpression of *Isl1* and *Ldb1* strongly promoted their expression. Thus, the *Isl1/Ldb1* complex plays a central role in transcriptional regulation and chromatin organization in three-dimensional space during cardiac differentiation and SHF development.

RESULTS

***Ldb1* regulates cardiac progenitor cell differentiation and second heart field development**

The LIM domain transcription factor *Isl1* is required for the proliferation, survival, and differentiation of SHF cardiac progenitor cells, as a consequence of which *Isl1*-deficient mouse embryos lack the right ventricle and the outflow tract, both structures derived from the SHF (Cai et al., 2003). Similarly, *Ldb1* deficiency results in early embryonic lethality with a series of developmental defects, including lack of heart formation (Mukhopadhyay et al., 2003). Therefore, we reasoned that *Isl1* and *Ldb1* might work in concert to regulate cardiac progenitor cell function. To elucidate the functional role of *Ldb1* in cardiogenesis we first utilized wild-type and *Ldb1* knockout (*Ldb1*^{-/-}) ES cells and differentiated them in embryoid bodies (EBs) to facilitate the generation and differentiation of cardiac progenitor cells (Figure 1A). Importantly, in contrast to control EBs, which started beating already at day 6 (d6), the EBs differentiated from *Ldb1*^{-/-} cells showed no beating foci (Figure 1B). Consistent with this, the expression of cardiomyocyte marker genes (*Mlc2a*, *Mlc2v*, *Tnnt2*) was dramatically reduced (Figure 1C). Additionally, the expression of endothelial markers (*Flk1*, *CD31*) was also downregulated (Figure

1C). By contrast, the expression of smooth muscle genes (*SM-actin*, *SM-22 α*) was upregulated (Figure 1C), suggesting that *Ldb1* is important for proper differentiation into cardiomyocyte and endothelial cell lineages. Next, we analyzed whether *Ldb1*-deficiency affects early developmental decisions, e.g. mesoderm induction, which could subsequently affect cardiac progenitor cell differentiation. Real-time PCR analysis for mesoderm (*Eomes*, *Bry*) and cardiac mesoderm markers (*Mesp1*, *Mesp2*) showed no significant difference in the peak expression level between control and *Ldb1*-deficient EBs, however the peak expression of these markers was delayed by one day (Figure 1D). Next, we analyzed the expression of pan-cardiac genes and genes specifically expressed in the FHF and the SHF (Figure 1E). Interestingly, while the expression of *Isl1*, *Tbx1*, *Hand2* and *Fgf10*, which play important roles in the SHF, and the pan-cardiac genes *Nkx2-5* and *Mef2c* was significantly downregulated at d4, d5 and d6, genes expressed in the FHF (*Tbx5*, *Hand1*, *Gata4*) showed no significant change (Figure 1E, data not shown), suggesting a role of *Ldb1* in the regulation of SHF progenitor cells. To further investigate the role of *Ldb1* in SHF development, we ablated *Ldb1* using an *Isl1-Cre* driver line that results in Cre recombination in SHF progenitor cells (Cai et al., 2003). *Isl1-Cre:Ldb1 flox/flox* embryos died by E10.5 with shortened outflow tract and small right ventricle (Figure 1F-G, Figure S1A). Furthermore, we observed significant downregulation of cardiomyocyte marker genes in the right ventricle and the outflow tract, both structures derived from the SHF, whereas no change in these genes was observed in the left ventricle, derived mainly from the first heart field (Figure 1H, Figure S1B). Taken together, these results confirm that *Ldb1* is essential for SHF progenitor cell differentiation and cardiac development.

Ldb1 protects *Isl1* from proteasomal degradation

To gain a better understanding of the mechanisms underlying *Ldb1* function in cardiogenesis, we analyzed cardiovascular progenitors in more detail. FACS analysis for Flk-1 and PdgfR- α demonstrated no significant differences in early cardiovascular progenitor numbers (Figure 2A). Interestingly, although *Isl1* mRNA levels were only slightly reduced in EBs differentiated from

Ldb1^{-/-} ES cells at all time-points that we analyzed (Figure 1E, 2B), *Isl1*⁺ cells were virtually absent in *Ldb1*^{-/-} EBs (Figure 2C). Western blot analysis confirmed the dramatically reduced levels of *Isl1* in *Ldb1*-deficient EBs (Figure 2D). The absence of *Isl1* protein, without pronounced changes of *Isl1* mRNA levels, suggested that *Isl1* is regulated at the protein level. Pull down of *Isl1* detected slower-migrating ubiquitinated forms of *Isl1*, that were increased in the presence of the proteasomal inhibitor MG-132, indicating that *Isl1* is targeted for proteasomal degradation (Figure 2E). To analyze this in more detail, we transfected HEK293T cells with *Isl1* deletion constructs lacking the LIM1 and/or LIM2 domain and treated them with MG-132. The levels of the truncated proteins lacking LIM2 or containing only the homeodomain were relatively unchanged, but the levels of the *Isl1* protein lacking LIM1 were significantly increased upon MG-132 treatment, suggesting that LIM2 is subjected to ubiquitination (Figure 2F). Next we analyzed whether binding of *Ldb1* to *Isl1* might protect it from proteasomal degradation, similarly to *Lhx3* (Gungor et al., 2007). To assess this possibility we transfected HEK293T cells with an *Isl1* plasmid alone or together with increasing amounts of *Ldb1* or *Ldb1* deletion constructs and constant amounts of GFP, which served as a control for transfection efficiency (Figure 2G). Importantly, increasing levels of *Ldb1* and truncated *Ldb1* protein lacking the dimerization domain (DN-*Ldb1*) led to a significant increase of *Isl1* protein levels but did not change the levels of truncated *Isl1* proteins lacking either the LIM1 or LIM2 domain, or harboring only the *Isl1* homeodomain (Figure 2G, 2H). Furthermore, a truncated *Ldb1* protein, lacking the LIM-interaction domain (LID), responsible for the interaction of *Isl1* with *Ldb1*, did not have an effect on *Isl1* protein levels (Figure 2G). Co-immunoprecipitations using *Isl1* deletion constructs revealed a critical role of the LIM1 domain of *Isl1* in mediating the interaction with *Ldb1* (Figure 2I), corroborating previous findings (Jurata et al., 1996). Together these data suggest that the binding of *Ldb1* to the LIM1 domain of *Isl1* protects it from ubiquitination at the LIM2 domain and subsequently from proteasomal degradation (Figure 7E).

Ldb1 and Isl1 physically, functionally and genetically interact to regulate cardiac progenitor cell differentiation and heart development

Ldb1 plays fundamental roles in development and cell differentiation as a cofactor for LIM-domain proteins, suggesting that Ldb1 and Isl1 might functionally interact with each other during cardiogenesis. To test this hypothesis, we first confirmed that Ldb1 and Isl1 interact in cardiac progenitor cells expressing endogenous levels of each protein by performing immunoprecipitation of Ldb1 from nuclear extracts of embryoid bodies (EBs) differentiated for 5 days, a stage enriched in cardiac progenitors. We found that Ldb1 was efficiently co-immunoprecipitated together with Isl1 (Figure 3A). Next, we transfected mouse ES cells with an expression plasmid carrying GFP alone or together with Isl1, Ldb1 or both Isl1 and Ldb1 (Figure S2A, S2B). GFP-expressing cells, isolated by FACS, were subjected to differentiation in EBs. Overexpression of Isl1 or Ldb1 alone significantly increased the percentage of beating EBs. Importantly, EBs differentiated from Isl1/Ldb1 overexpressing cells showed a higher number of beating foci compared to control EBs or EBs overexpressing Isl1 or Ldb1 alone, which had similar levels of Isl1 and Ldb1 compared to Isl1/Ldb1 overexpressing cells (Figure 3B, S2A, S2B). Consistently, the expression of the cardiomyocyte marker genes *Mlc2a* and *Mlc2v* was markedly increased and we observed a significant synergistic effect of Isl1 and Ldb1 on *Mlc2a* expression (Figure 3C). Furthermore, the expression of endothelial (*Flk1*, *VE-Cad*) and smooth muscle markers (*SM-actin*, *SM-Mhc*) was also increased (Figure 3D, 3E). Moreover, cardiac progenitor genes, which play key roles in SHF development (endogenous *Isl1*, *Mef2c*, *Hand2* and *Fgf10*) were significantly up-regulated (Figure 3F). Interestingly, overexpression of Ldb1 significantly increased Flk-1⁺PDGFR- α ⁺ cardiovascular progenitor numbers and the expression of Flk-1 and PDGFR- α (Figure 3G, Figure S2C), which may account for the increased expression of markers of all major cardiovascular lineages in Ldb1 and Isl1/Ldb1 overexpressing cells. Finally, we tested whether *Isl1* and *Ldb1* genetically interact during heart development. Crossing of *Isl1* heterozygous and *Ldb1* heterozygous mice revealed that only 5% of pups were

compound heterozygotes at the weaning stage, despite an expected ratio of 25%, whereas the other genotypes were recovered at similar percentages (Figure S2D). Timed mating revealed expected ratios of compound heterozygotes during mid to late gestation (Figure S2D), suggesting that the compound heterozygotes die after birth. Further histological analysis revealed that *Isl1/Ldb1* double haplodeficient embryos had various heart abnormalities, including a small and thin right ventricle, ventricular septal defect (VSD), overriding aorta (OA) and double outlet right ventricle (DORV) (Figure 3H-K). To analyze the primary cause of the observed heart defects we microdissected the heart and the SHF from wt, *Isl1*^{+/-}, *Ldb1*^{+/-} and *Isl1*^{+/-}*Ldb1*^{+/-} E9.25 embryos. Importantly, real-time PCR analysis revealed significant downregulation of *Hand2*, *Mef2c*, *Fgf10* and *Mlc2v* expression in *Isl1/Ldb1* double haplodeficient embryos, supporting a key role of *Isl1/Ldb1* complex in cardiomyocyte differentiation and *Mef2c*, *Hand2* and *Fgf10* expression (Figure 3L).

The dimerization domain of Ldb1 is required for SHF development and cardiac progenitor cell differentiation

To further investigate the functions of *Ldb1* during heart development, we ectopically overexpressed a truncated form of *Ldb1* lacking the dimerization domain (DN-*Ldb1*, Figure 2G, Figure S3A), by injecting mRNA into one-cell stage embryos of the zebrafish transgenic line *Tg(myf7:EGFP-HsHRAS)*^{s883}, which allows the easy monitoring of the cardiac morphology, through heart-specific expression of membrane-bound GFP (D'Amico et al., 2007). DN-*Ldb1* contains the highly conserved LIM-interaction domain (LID), which mediates high-affinity protein interactions with LIM domains, and can significantly stabilize *Isl1* protein levels (Figure 2G,H), but lacks the dimerization domain, necessary to promote long range promoter-enhancer interactions. It has been previously shown that overexpression of this mutant protein results in a competition with wild-type *Ldb* molecules for binding to LIM domains of LIM-HD proteins, acting in a dominant negative manner (Bach et al., 1999; Becker et al., 2002). Consistently with previous studies, the overexpression of DN-*Ldb1* led to defects in eye and brain development

(Figure S3B; (Becker et al., 2002)). Additionally, we observed that the heart contracted irregularly and with a reduced frequency (Figure S3C, S3D) in more than 80% of the embryos expressing DN-Ldb1. Furthermore the atrium of DN-Ldb1-expressing embryos was significantly shorter (Figure S3E). Interestingly, a similar phenotype was observed in *isl1*-mutant zebrafish embryos as a result of a failure of cardiomyocyte differentiation at the venous pole (de Pater et al., 2009). Confocal images of control and DN-Ldb1-expressing embryos stained with anti-*Isl1* antibodies at 48 hpf revealed dramatically less *Isl1*⁺ cardiomyocytes at the venous pole of the heart. In mutants, *Isl1*⁺ cells were found outside of the heart, but did not express the cardiomyocyte marker *myl7*, supporting a key role of Ldb1 dimerization in *Isl1*⁺ cardiomyocyte differentiation (Figure 4A). Consistent with this, *bmp4* expression in the sinus venosus was strongly reduced in DN-Ldb1-expressing embryos, although *bmp4* expression at the outflow pole and the atrioventricular canal was unaffected, in striking parallel to *isl1* mutant embryos (Figure 4B). Additionally, the expression of *mef2cb* was also downregulated (Figure 4C). Since *Isl1* plays a key role in cardiac progenitor cells during development, we further addressed whether this phenotype can be attributed to defects at early stages of cardiogenesis by performing *in situ* hybridization and whole mount anti-*Isl1* immunostaining of control and DN-Ldb1 overexpressing embryos at the 10 and 15 somites stage. No significant change of *isl1* mRNA expression was detected, suggesting that *Isl1*⁺ progenitor cell numbers were not changed in DN-Ldb1 injected embryos (Figure 4D). However, *Isl1* staining appeared to be stronger in the injected embryos, consistent with the stabilizing effect of DN-Ldb1 on *Isl1* protein levels (Figure 4D, Figure 2). Importantly, we observed strong downregulation of *hand2*, *mef2cb* and *nkx2-5*, which play important roles in the SHF development (Figure 4D), whereas no change was observed in *tbx5a* expression. These findings suggest that not only the stabilization of *Isl1* protein levels but also the formation of higher order complexes mediated by the Ldb1 dimerization domain might be important for proper cardiac progenitor cell differentiation during SHF development. To gain further support of this hypothesis, we generated stable Ldb1-deficient ES cell lines

overexpressing GFP alone, Isl1, Ldb1, DN-Ldb1 or in combinations. Consistent with an important role of Ldb1 in regulating Isl1 stability, Isl1 overexpressing *Ldb1*^{-/-} ES cells showed dramatically lower Isl1 protein levels, compared to *Ldb1*^{-/-} ES cells overexpressing Isl1 in combination with Ldb1 or the DN-Ldb1 (Figure S4A), although *Isl1* mRNA levels were similar (Figure S4B). Importantly, Ldb1 overexpression led to a rescue of cardiac differentiation, as measured by the increased percent of beating EBs and mRNA levels of cardiomyocyte marker genes, *Mlc2a*, *Mlc2v* and *Tnnt2* (Figure 4E, 4F). The functional rescue was further potentiated by overexpression of Isl1, confirming a synergistic role of these proteins in cardiomyocyte differentiation. By contrast, overexpression of DN-Ldb1 alone or in combination with Isl1 did not rescue the complete loss of cardiac differentiation of Ldb1-deficient EBs (Figure 4E, 4F). Furthermore, the expression of the endothelial marker genes *CD31* and *Flk1* was increased in *Ldb1*^{-/-} EBs overexpressing Ldb1, whereas smooth muscle genes were decreased by Ldb1 overexpression (Figure 4G), supporting a role of Ldb1 in the differentiation of cardiovascular progenitors into the cardiomyocyte and endothelial cell lineages and suppression of the smooth muscle lineage. FACS analysis for Flk-1 and Pdgfr- α showed no significant differences in the Flk-1⁺PDGFR- α ⁺ cardiovascular progenitor numbers upon Ldb1 and Isl1/Ldb1 overexpression in Ldb1-deficient EBs (Figure 4H), demonstrating that the dramatically increased cardiac differentiation is not due to an increased induction of cardiovascular progenitor cells. However, we observed a pronounced decrease of the Flk-1⁺/Pdgfr- α ⁺ population upon DN-Ldb1 expression (Figure 4H). Interestingly this decrease was rescued by Isl1 overexpression in combination with DN-Ldb1 (Figure 4H), suggesting that the decrease in cardiovascular progenitor cells upon DN-Ldb1 overexpression might be due to interference with the function of LIM only or LIM-HD proteins. Furthermore, we saw rescue of Isl1⁺ cells and Isl1 expression upon Ldb1 and DN-Ldb1 expression (Figure 4I, Figure S4C), consistent with the role of Ldb1 and DN-Ldb1 in stabilizing Isl1 protein levels, suggesting that the inability of DN-Ldb1 to rescue the cardiac differentiation defects of the Ldb1-deficient cells is not due to lack of Isl1⁺ cells.

Importantly, the expression of *Mef2c* and *Hand2*, factors crucial for SHF development and differentiation, was significantly upregulated upon Ldb1 overexpression but not upon overexpression of the DN-Ldb1 (Figure 4J). *Isl1* has been shown to directly bind to the anterior heart field (AHF) enhancer, which directs the expression of *Mef2c* in the AHF (Dodou et al., 2004, Witzel et al., 2012). Additionally, we found several conserved *Isl1* consensus motifs (YTAATGR; TAAKKR (Mazzoni et al., 2013)) between -1,5kb and the *Mef2c* transcription start site (Figure S5). Chromatin immunoprecipitation (ChIP) analysis of nuclear extracts from day 5 EBs demonstrated specific binding of *Isl1* and Ldb1 to the conserved *Isl1* binding sites (Figure 4K). Moreover, ChIP experiments in pools of E8-9 embryos showed strong enrichment of *Isl1* and Ldb1 at these sites (Figure 4L). Additionally, we found *Hand2* expression to be significantly altered upon loss and gain of function of Ldb1. *Hand2* plays a key role in SHF development (Srivastava et al., 1997; Tsuchihashi et al., 2011), and its expression in the heart is specifically driven by a cardiac-specific enhancer located between -4.5 kb and -2.7 kb of the *Hand2* transcription start site (Figure S6; OFTRV enhancer) (McFadden et al., 2000). *In silico* analysis revealed several *Isl1* consensus binding sites in the proximal promoter and the OFTRV enhancer of *Hand2* (Figure S6). ChIP analysis of d5 EBs and E8-9 embryos showed strong binding of both *Isl1* and Ldb1 at these sites (Figure 4M, 4N). Taken together, our data indicate that *Mef2c* and *Hand2* are direct targets of the *Isl1*/Ldb1 transcriptional complex.

Ldb1 facilitates long range enhancer-promoter interactions within the *Hand2* and *Mef2c* loci

Using chromosome conformation capture (3C) assays and 3C-based technologies (de Wit and de Laat, 2012; Dekker et al., 2002), it was shown that Ldb1 promotes chromatin looping events that bring distal enhancers into close proximity to promoters, thereby regulating gene expression (Deng et al., 2012; Morcillo et al., 1997; Soler et al., 2010; Song et al., 2007). To assess whether a similar mechanism controls cardiac progenitor cell gene expression, we analyzed whether binding of the *Isl1*/Ldb1 complex promotes chromatin loop formation at the

relatively small *Hand2* locus. Using 3C-qPCR analysis with the *Hand2* promoter as a viewpoint we observed a specific close proximity of the promoter with the OFTRV enhancer in d5 EBs from wild-type ES cells, but not in d5 EBs from *Ldb1*-deficient cells (Figure 5A). A similar interaction pattern was observed in *Ldb1*^{-/-} EBs overexpressing *Ldb1* and *Isl1/Ldb1* but not in EBs overexpressing DN-*Ldb1* or *Isl1/DN-Ldb1* (Figure 5A, Figure S7A). No interaction was observed between the promoter and negative regions for *Isl1* and *Ldb1* binding located upstream of the OFTRV enhancer, between the promoter and OFTRV enhancer and downstream of the promoter. Further, no interaction was detected in wild-type and *Ldb1*-deficient ES cells, which do not express *Isl1* (Figure 5A, Figure S7A).

Next, to characterize the spatial interactions within the *Mef2c* locus we performed 3C-seq (Stadhouders et al., 2013), using two viewpoints: the *Mef2c* AHF enhancer, which drives *Mef2c* expression specifically in the AHF and the *Mef2c* promoter which drives *Mef2c* expression in different cell types. Multiple promoter-interacting elements were detected in the *Mef2c* locus, of which some showed a lower signal in *Ldb1*-deficient EBs (Figure 5B). Importantly, we observed interactions of the AHF enhancer with the promoter area and with the 3' end of the *Mef2c* gene, which were decreased in *Ldb1*-deficient EBs (Figure 5B). 3C-qPCR experiments revealed a similar long-range interaction pattern in wild-type versus *Ldb1*^{-/-} EBs during the course of cardiac differentiation, as well as from dissected SHF and hearts of E8-10.5 embryos, confirming the 3C-seq results (Figure 5C). Interestingly, we observed interactions of the AHF enhancer with the *Mef2c* proximal promoter co-occupied by *Isl1* and *Ldb1* in d4 EBs at the onset of *Mef2c* expression and in dissected SHF of E8.5 embryos, whereas in d5 EBs and dissected hearts from E9.5-10.5 embryos we observed strong interactions with regions more distal to the transcription start site (Figure 5C-D). Additionally, no interactions of the AHF enhancer with the promoter and with the 3' end of the *Mef2c* gene was observed in the tail of the E8-9 embryos, suggesting that these chromatin loops are specifically formed in cardiac progenitor cells. Importantly, the 3C-seq signals correlated with the binding of *Isl1* and *Ldb1* at the *Mef2c* locus

(Figure S7B). Next, we sought to analyze whether the Ldb1 dimerization domain is required for chromatin loop formation by performing 3C-qPCR in d4 and d5 EBs from *Ldb1*^{-/-} ES cells overexpressing Isl1, Ldb1 and DN-Ldb1 alone or in combinations. Using the AHF enhancer as a viewpoint we observed a specific interaction of the AHF enhancer with the *Mef2c* promoter and the 3' end of *Mef2c* gene in *Ldb1*^{-/-} EBs overexpressing Ldb1 and Isl1/Ldb1, but observed no interaction of these genomic regions in *Ldb1*^{-/-} EBs overexpressing DN-Ldb1 and Isl1/DN-Ldb1 (Figure 5D). To analyze, whether the inability of DN-Ldb1 to promote loop formation was due to its inability to bind to the Isl1/Ldb1 binding sites we performed ChIP analysis of *Ldb1*^{-/-} ES cells overexpressing Isl1 alone or in combinations with HA-Ldb1 or HA-DN-Ldb1 using anti-HA antibody. Importantly, we observed similar enrichment of Ldb1 and DN-Ldb1 at the *Mef2c* promoter and AHF enhancer, showing that the DN-Ldb1/Isl1 complex binds at its target sites, but cannot promote long-range promoter-enhancer interactions, necessary for proper gene regulation (Figure S7C). Finally, luciferase assays revealed significant synergistic effect of Isl1 and Ldb1 on a luciferase construct containing the *Mef2c* promoter upstream and the *Mef2c* AHF enhancer downstream of a luciferase gene, in comparison to a reporter construct harboring the *Mef2c* promoter alone (Figure S7D), suggesting the requirement of Isl1/Ldb1 complexes in promoting long range promoter enhancer interactions to ensure high levels of heart specific *Mef2c* expression.

To understand the functional significance of the dynamic chromatin looping at the *Mef2c* locus during the course of cardiac progenitor cell differentiation and heart development we analyzed the expression of annotated alternative *Mef2c* transcripts. Interestingly, while the longer reference sequence transcript (Refseq) was highly expressed in d4 EBs and in dissected SHF, the transcript with alternative transcriptional start site 1.5 kb downstream of the AHF enhancer was more abundant later during EB differentiation and in dissected hearts (Figure 5E), implying that the observed dynamic chromatin looping correlates with the expression of alternative transcripts for *Mef2c*. To better characterize the -14 kb to -5.5 kb genomic region found in close

proximity to the AHF enhancer we screened this region for known enhancer-associated chromatin marks H3K27ac, H3K4me1, p300 and Pol II. We found a marked enrichment of these marks -13 kb upstream of the TSS, which correlated with strong binding of Isl1 and Ldb1 at these sites (Figure 5F, Figure S7B). Sites within the -14 kb to -5.5 kb genomic region which were not bound by Isl1 and Ldb1 did not show significant enrichment of enhancer-associated chromatin marks (Figure 5F).

Ldb1 orchestrate a network for transcriptional regulation and coordination in three-dimensional space during cardiogenesis

Gene Ontology (GO) analysis of sequences found by the 3C-seq in close proximity to the AHF enhancer over-represented in wild-type versus *Ldb1*^{-/-} EBs, showed an enrichment of genes involved in heart development, cardiac muscle development, cell fate commitment and vasculature development within the first ten most enriched GO terms (Figure 6A, p<0.01). By contrast, when similar analysis was performed using the sequences found in proximity to the *Mef2c* promoter, no overrepresentation of GO terms involved in heart development was observed (Figure 6B). Importantly, we found that the AHF enhancer is involved in contacts with multiple genes, which play key roles during cardiac progenitor cell differentiation and heart development (Figure 6C, Table S1). 3C-qPCR analysis of wild-type versus *Ldb1*^{-/-} EBs, as well as of dissected SHF or tails of E8-9 embryos confirmed the specificity and the Ldb1-dependence of these interactions (Figure 6D, 6E). Importantly, in d4 and d6 *Ldb1*-deficient EBs we observed significant downregulation of selected genes, which show significantly higher association with the AHF enhancer in wild-type versus *Ldb1*^{-/-} EBs (Figure 7A). By contrast, genes which showed similar association with the AHF enhancer in wild-type and *Ldb1*^{-/-} EBs (*Rai2*, *Xrcc4*), were not altered. Furthermore, overexpression of Isl1 and Ldb1, but not DN-Ldb1 strongly promoted the expression of the genes that were highly associated with the AHF enhancer in wild type EBs (Figure 7B). Moreover, we observed significant downregulation of these genes in hearts and dissected SHF regions of *Isl1*^{+/-}/*Ldb1*^{+/-} E9.25 embryos compared to wild-type

embryos (Figure 7C, 7D). Taken together, these data provide strong support for a model according to which the Isl1/Ldb1-containing transcription complexes orchestrate a network for transcriptional regulation and coordination in three-dimensional space to regulate cardiac progenitor cell differentiation and heart development (Figure 7E).

DISCUSSION

The differentiation of cardiac progenitor cells into distinct lineages involves a coordinated series of large-scale transcriptional changes, but how these events are coordinated at the molecular level has remained poorly understood. Our study shows that a complex between the central SHF transcription factor Isl1 and the multi-adaptor protein Ldb1 plays a crucial role in directing chromatin organization and coordinating a cardiac lineage specific gene expression program.

We found that Ldb1-deficient ES cells show a markedly decreased expression of SHF marker genes and subsequently impaired differentiation into the cardiomyocyte and endothelial lineages, while differentiation into the smooth muscle lineage was increased. Ldb1 gain-of-function experiments confirmed the requirement of Ldb1 in the differentiation of cardiovascular progenitors in cardiomyocytes and endothelial cells and in suppressing the smooth muscle lineage. FACS analysis for Flk-1 and PdgfR- α and qPCR for *Mesp1/2* revealed no significant differences in cardiovascular progenitor numbers upon Ldb1-deficiency, suggesting that Ldb1 loss affects the differentiation of cardiovascular progenitor cells, but not cardiogenic cell-lineage commitment. Interestingly however, overexpression of Ldb1 in wild-type EBs significantly increased the number of Flk-1+PDGFR- α + cardiovascular progenitors, suggesting that modulation of Ldb1 levels might affect cardiac lineage commitment. Consistent with this, of DN-Ldb1, which competes with full-length Ldb1 for binding to LIM domain proteins led to a significant decrease in Flk-1⁺PdgfR- α ⁺ cardiovascular progenitor cells, implying functional redundancy between Ldb1 and Ldb2 in cardiac lineage commitment. Mechanistically, we show that the importance of Ldb1 for cardiac differentiation and SHF development is two-fold (Figure 7E): (i)

Ldb1 binds to Isl1 and protects it from proteasomal degradation, as a consequence of which Ldb1-deficiency leads to an almost complete loss of Isl1+ cardiovascular progenitor cells. We found that Isl1 is ubiquitinated at its LIM2 domain and via the binding of Ldb1, mainly to LIM1, Ldb1 protects Isl1 from degradation. This is consistent with previous studies, showing that LIM-HD proteins levels are regulated by the proteasome and that binding of Ldb1 to LIM domain proteins protects them from degradation (Gungor et al., 2007). (ii) The Isl1/Ldb1 complex orchestrates a network for transcriptional regulation and coordination in three-dimensional space driving cardiac differentiation and heart development. A truncated Ldb1 protein (DN-Ldb1), which contains the LIM interaction domain and thereby can protect Isl1 protein from degradation, but lacks the dimerization domain and thus cannot promote long-range enhancer-promoter interactions (Krivega et al., 2014) did not collaborate with Isl1 to regulate the expression of their common targets and failed to rescue the cardiac differentiation defects of Ldb1-deficient cells (Figure 4E-F). Importantly, overexpression of DN-Ldb1 in zebrafish embryos leads to defects in the differentiation of Isl1+ cardiac progenitors at the venous pole in striking parallel with *Isl1* mutant fishes (de Pater et al., 2009), presumably by competing with full-length Ldb1 for binding to Isl1 (Bach et al., 1999). Importantly, upon overexpression of DN-Ldb1 we observed significant downregulation of *hand2* and *mef2cb*, transcription factors which play important roles in cardiomyocyte differentiation and heart development (Lin et al., 1997; Srivastava et al., 1997; Tsuchihashi et al., 2011). Similarly, we observed decreased expression of *Hand2* and *Mef2c* in *Ldb1*-deficient EBs, which showed complete blockade of cardiomyocyte differentiation, and in *Isl1/Ldb1* haplodeficient embryos, which developed various cardiac anomalies. Moreover, our results suggest that the Isl1/Ldb1 complex directly regulates *Mef2c* and *Hand2* expression by binding to their heart specific enhancers and stimulating promoter-enhancer interactions. Similarly, Ldb1 is required for the looping of the β -globin locus control region (LCR) to the β -globin promoter (Deng et al., 2012; Song et al., 2007; Tolhuis et al., 2002), and it was shown that a fusion protein of LMO2 and the Ldb1 dimerization domain is sufficient to restore looping of

the β -globin promoter to the LCR and transcription in Ldb1 knockdown cells (Krivega et al., 2014).

Mef2c plays a key role in regulating anterior heart field development and cardiomyocyte differentiation. Similarly to *Isl1*, *Mef2c*-deficient hearts show outflow tract abnormalities and fail to form the right ventricle (Cai et al., 2003; Lin et al., 1997). 3C-seq and 3C-qPCR using the AHF enhancer of *Mef2c*, which confers responsiveness to *Isl1* and GATA factors (Dodou et al., 2004), as a viewpoint identified close proximity between the promoter region, the AHF enhancer and the 3' end of the gene. Gene looping has been shown to bring promoter and terminator regions together in close proximity in the early stages of transcriptional activation, facilitating RNA pol II re-initiation and high-level expression of the long genes *FMP27* and *SEN1* in *Saccharomyces cerevisiae* (O'Sullivan et al., 2004). Similarly, the observed loop between the promoter and the 3' end of the *Mef2c* gene could generate a functional re-initiation complex for subsequent rounds of *Mef2c* transcription. Further, we observed dynamic chromatin looping at the *Mef2c* locus during heart development and in the course of cardiac progenitor cell differentiation, in which the AHF enhancer contacts the proximal promoter during the onset of *Mef2c* gene activation in the anterior heart field, whereas later this contact is lost, correlating with the expression of an alternative transcript with TSS 1.5 kb downstream of the AHF enhancer. A similar developmental switch in chromatin looping was observed during erythroid differentiation at the *β -globin* locus, from favoring the expression of embryonic globin genes in erythroid progenitors to favoring the expression of the adult globin genes in definitive erythrocytes (Palstra et al., 2003).

Remarkably, our 3C-seq data identified surprisingly specific, Ldb1-mediated interactions of the AHF enhancer with multiple genes that play key roles in cardiovascular development, as well as cell fate commitment, suggesting a role of Ldb1 in regulating a cardiac-specific interaction network around the *Mef2c* AHF enhancer. These interactions are cell type specific, as they were observed in cardiac cells but not in other cells types, and are lost upon Ldb1-deficiency. Recent studies analyzing enhancer contacts during *Drosophila* development, revealed that a large

number of enhancer interactions are unchanged between different tissues and developmental stages and only few of them show significant changes (Ghavi-Helm et al., 2014). Notably, Ldb1 appears to mediate cardiac cell-type specific chromatin loops and transcriptional programs, via its diverse DNA binding partners (Figure 5-7, (Soler et al., 2010; Song et al., 2007; Tolhuis et al., 2002)). Importantly, Ldb1 deficiency led to dramatically decreased expression of the genes associated with the AHF enhancer and overexpression of *Isl1* and Ldb1 strongly promoted their expression. The dosage-sensitive interdependence between *Isl1* and Ldb1 in the expression of these key factors in cardiogenesis, further supports a key role of the *Isl1/Ldb1* complex in coordinating chromatin looping and heart-specific gene expression. Notably, we observed significant enrichment for binding of the core cardiac transcription factors Gata-s, Nkx2-5, Mef2c and Tbx-s (Figure S7E) within the genomic regions found in close proximity to the *Mef2c* AHF enhancer. Interestingly, co-occupancy of these factors identifies transcriptional enhancers active in the heart (He et al., 2011) and their overexpression leads to a direct reprogramming of fibroblasts into functional cardiomyocytes, further supporting a role of cell type-specific transcription factor-regulatory networks in the control of cell type-specific genome organization and gene expression (de Wit et al., 2013; Denholtz et al., 2013).

In conclusion, our study highlights a central role for Ldb1 in regulating cardiac progenitor cell differentiation and SHF development and provides exciting novel insights into the molecular machinery that orchestrates chromatin organization and coordinated gene expression during cardiogenesis.

EXPERIMENTAL PROCEDURES

Plasmids and Antibodies

For detailed plasmid information, see the Supplemental Experimental Procedures. The following primary antibodies were used: rabbit anti-HA (Y-11; Santa Cruz Biotechnology), mouse anti-Flag (M2, Sigma), goat anti-Ldb1 (N-18, Santa Cruz Biotechnology), mouse anti-Ldb1 (C-9 Santa

Cruz Biotechnology), mouse anti-Islet1 39.4D5 (Developmental Studies Hybridoma Bank); goat anti-Lamin B (C-20; Santa Cruz Biotechnology), mouse anti-tubulin (T5168 Sigma), anti-GFP (ab6556 Abcam), APC-conjugated anti-Flk1 (e-Bioscience 17-5821-81) and PE-conjugated anti-PDGFR α (e-Bioscience 12-1401-81).

Immunoprecipitation and ChIP

Co-IPs and ChIP was performed as described in (Witzel et al., 2012). Detailed protocols are described in Supplemental Experimental Procedures.

RNA Isolation, RT-PCR, and Real-Time PCR

Embryos were dissected, and the SHF region and the heart were separately collected in cold PBS. RNA from EBs and embryos was isolated using Trizol (Invitrogen). cDNA was synthesized with the High Capacity cDNA Reverse Transcription Kit (Applied Biosystems) and real-time PCR was performed using the SYBR GREEN PCR master mix (Applied Biosystems) on Applied Biosystems StepOnePlusTM real-time PCR detection system.

Chromosome Conformation Capture Assays - 3C-seq and 3C-qPCR

3C-seq and 3C-qPCR was performed as described in (Stadhouders et al., 2013). In brief, 1×10^7 cells or dissected SHF regions or tails of 20 E8-9 embryos were crosslinked with 2% formaldehyde at room temperature for 10 min, followed by glycine quenching, cell lysis, HindIII (for 3C-seq and 3C-qPCR of the *Mef2c* locus) or NlaIII (or DpnII) digestion (3C-qPCR of the *Hand2* locus), and T4 ligation. As a positive control genomic DNA or bacterial artificial chromosomes (BAC) containing the entire *Mef2c* and *Hand2* loci (Invitrogen) digested with HindIII or NlaIII (or DpnII) respectively were used, and religated to generate random ligation products. Primers sequences are listed in the Supplemental Experimental Procedures.

Zebrafish strains

Embryos and adult zebrafish were raised under standard laboratory conditions at 28 °C. The following mutant and transgenic lines were used: *Tg(myf17:EGFP-HsHRAS)^{s883}* (D'Amico et al., 2007) and *isl1sa0029* (Sanger Institute, Zebrafish Mutation Resource).

Mouse lines

The Ldb1^{tm1a(EUCOMM)Wtsi} line was generated by microinjection of Ldb1^{tm1a(EUCOMM)Wtsi} ES cells, obtained from the European Conditional Mouse Mutagenesis Program (EUCOMM), into blastocysts.

mRNA injection

mRNA synthesis was performed using mMESSAGE mMACHINE® SP6 Transcription Kit (Ambion) following manufacturer's instructions. mRNA was injected in 1- cell stage of fertilized zebrafish eggs (volume 2 nl, mRNA concentration 200 ng/μl for Flag-HA-DN-Ldb1).

***In situ* hybridization, whole mount immunostaining and confocal microscopy**

In situ hybridization and whole-mount staining was performed as described (Witzel et al., 2012). Confocal images were acquired by a Zeiss LSM 710 system and the Z-stacks were projected by Zeiss LSM 710 software.

Data deposition

All sequencing data have been deposited in GEO (accession number SRP055800).

SUPPLEMENTAL INFORMATION

Supplemental Information includes Supplemental Experimental Procedures, seven figures and two tables.

ACKNOWLEDGMENTS

We thank Ingrid Konrad, Susanne Kreutzer, Kerstin Richter and Monika Müller-Boche for technical assistance. We are grateful to Boyan Garvalov, for carefully reading the manuscript and the constructive comments. This work was supported by the LOEWE Center for Cell and Gene Therapy (CGT) and the LOEWE Universities of Giessen and Marburg Lung Center (UGMLC), financed by the Hessian Ministry of Higher Education, Research and the Arts (III L 4-518/17.004 (2013)) and an Emmy-Noether Program grant DO 1323/1-1, the SFB TRR 81 and the Excellence Cluster Cardio-Pulmonary System EXC 147 of the DFG (Germany).

REFERENCES

- Aguirre, A., Sancho-Martinez, I., and Izpisua Belmonte, J.C. (2013). Reprogramming toward heart regeneration: stem cells and beyond. *Cell Stem Cell* *12*, 275-284.
- Bach, I., Carriere, C., Ostendorff, H.P., Andersen, B., and Rosenfeld, M.G. (1997). A family of LIM domain-associated cofactors confer transcriptional synergism between LIM and Otx homeodomain proteins. *Genes Dev* *11*, 1370-1380.
- Bach, I., Rodriguez-Esteban, C., Carriere, C., Bhushan, A., Kronen, A., Rose, D.W., Glass, C.K., Andersen, B., Izpisua Belmonte, J.C., and Rosenfeld, M.G. (1999). RLIM inhibits functional activity of LIM homeodomain transcription factors via recruitment of the histone deacetylase complex. *Nat Genet* *22*, 394-399.
- Becker, T., Ostendorff, H.P., Bossenz, M., Schluter, A., Becker, C.G., Peirano, R.I., and Bach, I. (2002). Multiple functions of LIM domain-binding CLIM/NLI/Ldb cofactors during zebrafish development. *Mechanisms of development* *117*, 75-85.
- Cai, C.L., Liang, X., Shi, Y., Chu, P.H., Pfaff, S.L., Chen, J., and Evans, S. (2003). *Isl1* identifies a cardiac progenitor population that proliferates prior to differentiation and contributes a majority of cells to the heart. *Dev Cell* *5*, 877-889.
- D'Amico, L., Scott, I.C., Jungblut, B., and Stainier, D.Y. (2007). A mutation in zebrafish *hmgcr1b* reveals a role for isoprenoids in vertebrate heart-tube formation. *Current biology : CB* *17*, 252-259.
- de Pater, E., Clijsters, L., Marques, S.R., Lin, Y.F., Garavito-Aguilar, Z.V., Yelon, D., and Bakkers, J. (2009). Distinct phases of cardiomyocyte differentiation regulate growth of the zebrafish heart. *Development* *136*, 1633-1641.
- de Wit, E., Bouwman, B.A.M., Zhu, Y., Klous, P., Splinter, E., Versteegen, M.J.A.M., Krijger, P.H.L., Festuccia, N., Nora, E.P., Welling, M., *et al.* (2013). The pluripotent genome in three dimensions is shaped around pluripotency factors. *Nature* *501*, 227-+.
- de Wit, E., and de Laat, W. (2012). A decade of 3C technologies: insights into nuclear organization. *Genes Dev* *26*, 11-24.
- Dekker, J., Rippe, K., Dekker, M., and Kleckner, N. (2002). Capturing chromosome conformation. *Science* *295*, 1306-1311.
- Deng, W., Lee, J., Wang, H., Miller, J., Reik, A., Gregory, P.D., Dean, A., and Blobel, G.A. (2012). Controlling long-range genomic interactions at a native locus by targeted tethering of a looping factor. *Cell* *149*, 1233-1244.
- Denholtz, M., Bonora, G., Chronis, C., Splinter, E., de Laat, W., Ernst, J., Pellegrini, M., and Plath, K. (2013). Long-range chromatin contacts in embryonic stem cells reveal a role for pluripotency factors and polycomb proteins in genome organization. *Cell Stem Cell* *13*, 602-616.
- Dixon, J.R., Jung, I., Selvaraj, S., Shen, Y., Antosiewicz-Bourget, J.E., Lee, A.Y., Ye, Z., Kim, A., Rajagopal, N., Xie, W., *et al.* (2015). Chromatin architecture reorganization during stem cell differentiation. *Nature* *518*, 331-336.
- Dixon, J.R., Selvaraj, S., Yue, F., Kim, A., Li, Y., Shen, Y., Hu, M., Liu, J.S., and Ren, B. (2012). Topological domains in mammalian genomes identified by analysis of chromatin interactions. *Nature* *485*, 376-380.
- Dodou, E., Verzi, M.P., Anderson, J.P., Xu, S.M., and Black, B.L. (2004). *Mef2c* is a direct transcriptional target of *ISL1* and *GATA* factors in the anterior heart field during mouse embryonic development. *Development* *131*, 3931-3942.

- Evans, S.M., Yelon, D., Conlon, F.L., and Kirby, M.L. (2010). Myocardial lineage development. *Circ Res* *107*, 1428-1444.
- Ghavi-Helm, Y., Klein, F.A., Pakozdi, T., Ciglar, L., Noordermeer, D., Huber, W., and Furlong, E.E. (2014). Enhancer loops appear stable during development and are associated with paused polymerase. *Nature* *512*, 96-100.
- Gorkin, D.U., Leung, D., and Ren, B. (2014). The 3D genome in transcriptional regulation and pluripotency. *Cell Stem Cell* *14*, 762-775.
- Gungor, C., Taniguchi-Ishigaki, N., Ma, H., Drung, A., Tursun, B., Ostendorff, H.P., Bossenz, M., Becker, C.G., Becker, T., and Bach, I. (2007). Proteasomal selection of multiprotein complexes recruited by LIM homeodomain transcription factors. *Proc Natl Acad Sci U S A* *104*, 15000-15005.
- Hansson, E.M., Lindsay, M.E., and Chien, K.R. (2009). Regeneration next: toward heart stem cell therapeutics. *Cell Stem Cell* *5*, 364-377.
- He, A., Kong, S.W., Ma, Q., and Pu, W.T. (2011). Co-occupancy by multiple cardiac transcription factors identifies transcriptional enhancers active in heart. *Proc Natl Acad Sci U S A* *108*, 5632-5637.
- Jurata, L.W., Kenny, D.A., and Gill, G.N. (1996). Nuclear LIM interactor, a rhombotin and LIM homeodomain interacting protein, is expressed early in neuronal development. *Proc Natl Acad Sci U S A* *93*, 11693-11698.
- Jurata, L.W., Pfaff, S.L., and Gill, G.N. (1998). The nuclear LIM domain interactor NLI mediates homo- and heterodimerization of LIM domain transcription factors. *J Biol Chem* *273*, 3152-3157.
- Kagey, M.H., Newman, J.J., Bilodeau, S., Zhan, Y., Orlando, D.A., van Berkum, N.L., Ebmeier, C.C., Goossens, J., Rahl, P.B., Levine, S.S., *et al.* (2010). Mediator and cohesin connect gene expression and chromatin architecture. *Nature* *467*, 430-435.
- Krivega, I., Dale, R.K., and Dean, A. (2014). Role of LDB1 in the transition from chromatin looping to transcription activation. *Genes Dev* *28*, 1278-1290.
- Kwon, C., Qian, L., Cheng, P., Nigam, V., Arnold, J., and Srivastava, D. (2009). A regulatory pathway involving Notch1/beta-catenin/Isl1 determines cardiac progenitor cell fate. *Nat Cell Biol* *11*, 951-957.
- Laflamme, M.A., and Murry, C.E. (2011). Heart regeneration. *Nature* *473*, 326-335.
- Lin, Q., Schwarz, J., Bucana, C., and Olson, E.N. (1997). Control of mouse cardiac morphogenesis and myogenesis by transcription factor MEF2C. *Science* *276*, 1404-1407.
- Mazzoni, E.O., Mahony, S., Closser, M., Morrison, C.A., Nedelec, S., Williams, D.J., An, D., Gifford, D.K., and Wichterle, H. (2013). Synergistic binding of transcription factors to cell-specific enhancers programs motor neuron identity. *Nature neuroscience* *16*, 1219-1227.
- McFadden, D.G., Charite, J., Richardson, J.A., Srivastava, D., Firulli, A.B., and Olson, E.N. (2000). A GATA-dependent right ventricular enhancer controls dHAND transcription in the developing heart. *Development* *127*, 5331-5341.
- Meier, N., Krpic, S., Rodriguez, P., Strouboulis, J., Monti, M., Krijgsveld, J., Gering, M., Patient, R., Hostert, A., and Grosveld, F. (2006). Novel binding partners of Ldb1 are required for haematopoietic development. *Development* *133*, 4913-4923.
- Morcillo, P., Rosen, C., Baylies, M.K., and Dorsett, D. (1997). Chip, a widely expressed chromosomal protein required for segmentation and activity of a remote wing margin enhancer in *Drosophila*. *Genes Dev* *11*, 2729-2740.
- Moretti, A., Caron, L., Nakano, A., Lam, J.T., Bernshausen, A., Chen, Y., Qyang, Y., Bu, L., Sasaki, M., Martin-Puig, S., *et al.* (2006). Multipotent embryonic *isl1*⁺ progenitor cells lead to cardiac, smooth muscle, and endothelial cell diversification. *Cell* *127*, 1151-1165.

- Mukhopadhyay, M., Teufel, A., Yamashita, T., Agulnick, A.D., Chen, L., Downs, K.M., Schindler, A., Grinberg, A., Huang, S.P., Dorward, D., *et al.* (2003). Functional ablation of the mouse *Ldb1* gene results in severe patterning defects during gastrulation. *Development* *130*, 495-505.
- O'Sullivan, J.M., Tan-Wong, S.M., Morillon, A., Lee, B., Coles, J., Mellor, J., and Proudfoot, N.J. (2004). Gene loops juxtapose promoters and terminators in yeast. *Nat Genet* *36*, 1014-1018.
- Palstra, R.J., Tolhuis, B., Splinter, E., Nijmeijer, R., Grosveld, F., and de Laat, W. (2003). The beta-globin nuclear compartment in development and erythroid differentiation. *Nat Genet* *35*, 190-194.
- Peric-Hupkes, D., Meuleman, W., Pagie, L., Bruggeman, S.W., Solovei, I., Brugman, W., Graf, S., Flicek, P., Kerkhoven, R.M., van Lohuizen, M., *et al.* (2010). Molecular maps of the reorganization of genome-nuclear lamina interactions during differentiation. *Mol Cell* *38*, 603-613.
- Phillips-Cremins, J.E., Sauria, M.E., Sanyal, A., Gerasimova, T.I., Lajoie, B.R., Bell, J.S., Ong, C.T., Hookway, T.A., Guo, C., Sun, Y., *et al.* (2013). Architectural protein subclasses shape 3D organization of genomes during lineage commitment. *Cell* *153*, 1281-1295.
- Shen, Y., Yue, F., McCleary, D.F., Ye, Z., Edsall, L., Kuan, S., Wagner, U., Dixon, J., Lee, L., Lobanenkov, V.V., *et al.* (2012). A map of the cis-regulatory sequences in the mouse genome. *Nature* *488*, 116-120.
- Soler, E., Andrieu-Soler, C., de Boer, E., Bryne, J.C., Thongjuea, S., Stadhouders, R., Palstra, R.J., Stevens, M., Kockx, C., van Ijcken, W., *et al.* (2010). The genome-wide dynamics of the binding of *Ldb1* complexes during erythroid differentiation. *Genes Dev* *24*, 277-289.
- Song, S.H., Hou, C., and Dean, A. (2007). A positive role for *NLI/Ldb1* in long-range beta-globin locus control region function. *Mol Cell* *28*, 810-822.
- Srivastava, D., Thomas, T., Lin, Q., Kirby, M.L., Brown, D., and Olson, E.N. (1997). Regulation of cardiac mesodermal and neural crest development by the bHLH transcription factor, dHAND. *Nat Genet* *16*, 154-160.
- Stadhouders, R., Kolovos, P., Brouwer, R., Zuin, J., van den Heuvel, A., Kockx, C., Palstra, R.J., Wendt, K.S., Grosveld, F., van Ijcken, W., *et al.* (2013). Multiplexed chromosome conformation capture sequencing for rapid genome-scale high-resolution detection of long-range chromatin interactions. *Nature protocols* *8*, 509-524.
- Tolhuis, B., Palstra, R.J., Splinter, E., Grosveld, F., and de Laat, W. (2002). Looping and interaction between hypersensitive sites in the active beta-globin locus. *Mol Cell* *10*, 1453-1465.
- Tripic, T., Deng, W., Cheng, Y., Zhang, Y., Vakoc, C.R., Gregory, G.D., Hardison, R.C., and Blobel, G.A. (2009). SCL and associated proteins distinguish active from repressive GATA transcription factor complexes. *Blood* *113*, 2191-2201.
- Tsuchihashi, T., Maeda, J., Shin, C.H., Ivey, K.N., Black, B.L., Olson, E.N., Yamagishi, H., and Srivastava, D. (2011). *Hand2* function in second heart field progenitors is essential for cardiogenesis. *Dev Biol* *351*, 62-69.
- Vincent, S.D., and Buckingham, M.E. (2010). How to make a heart: the origin and regulation of cardiac progenitor cells. *Curr Top Dev Biol* *90*, 1-41.
- Witzel, H.R., Jungblut, B., Choe, C.P., Crump, J.G., Braun, T., and Dobрева, G. (2012). The LIM protein *Ajuba* restricts the second heart field progenitor pool by regulating *Isl1* activity. *Dev Cell* *23*, 58-70.

FIGURE LEGENDS

Figure 1. Ablation of *Ldb1* results in defects in cardiac progenitor cell differentiation and SHF development. (A) Schematic diagram of the experimental setup. (B) Percentage of beating EBs in wild-type and *Ldb1*^{-/-} ES cells differentiated in EBs. (C) Relative mRNA expression of cardiomyocyte (*Mlc2a*, *Mlc2v*, *Tnnt2*), endothelial (*Flk1*, *CD31*) and smooth muscle (*SM-actin*, *SM-22α*) genes in d9 EBs differentiated from wild-type and *Ldb1*^{-/-} ES cells. (D) Relative mRNA expression of mesodermal markers (*Eomes*, *Bry*, *Mesp1* and *Mesp2*) in EBs differentiated from control and *Ldb1*^{-/-} ES cells at different days. (E) Relative mRNA expression of cardiac progenitor marker genes in d4 EBs differentiated from *Ldb1*^{+/+} and *Ldb1*^{-/-} ES cells. (F) Gross appearance of control (*Isl1*^{cre/+}/*Ldb1*^{+/*flox*}) and *Isl1*^{cre/+}/*Ldb1*^{flox/flox} embryos at E10.5, showing developmental arrest of the *Ldb1*-deficient embryos. Scale bars, 500 μm. (G) Higher magnification of E9.5 embryos viewed from the right (left panels) and the front (right panels), showing a short outflow tract and a small right ventricle. Scale bars, 200 μm. Abbreviations: OFT, outflow tract; RV, right ventricle; LV, left ventricle. (H) Relative mRNA expression analysis of cardiomyocyte genes in dissected outflow tract and right ventricle of E9.25 wild-type and *Isl1*^{cre/+}/*Ldb1*^{flox/flox} embryos. Data are mean ± SEMs, n=3 for each genotype. See also Figure S1.

Figure 2. *Ldb1* binds to *Isl1* and protects it from proteasomal degradation. (A) FACS analysis of *Flk-1* and *PdgfR-α* expression in d3.75 EBs differentiated from control and *Ldb1*^{-/-} ES cells (B) Relative mRNA expression of *Isl1* in EBs differentiated from control and *Ldb1*^{-/-} ES cells at different days. (C) *Isl1* immunostaining on vibratome sections from d5 EBs differentiated from control and *Ldb1*^{-/-} ES cells. Scale bars, 100 μm. (D) Western blot analysis of total protein extracts of day 4, 5 and 6 EBs differentiated from control and *Ldb1*^{-/-} ES cells. Lamin B1 served as loading control. (E) HA-tagged ubiquitin and *Isl1* were transiently expressed in HEK293T cells. Cells were either treated with DMSO or with MG-132 6 h before harvesting. Equivalent amounts of total cellular protein were immunoprecipitated with an anti-*Isl1* antibody. The co-

immunoprecipitated proteins were detected by an immunoblot analysis with an anti-HA antibody. **(F)** Schematic representation of wild-type *Isl1* and *Isl1* deletion constructs, lacking either LIM1 or LIM2 or harboring only the homeodomain (top). Western blot analysis of whole cell lysates of HEK293T cells transfected with *Isl1*, *Isl1* Δ LIM1, *Isl1* Δ LIM2 and *Isl1*Homeo expression plasmids, treated with DMSO or MG-132. **(G)** Schematic representation of wild-type *Ldb1* and *Ldb1* deletion constructs. *Ldb1* harbors three domains that have been shown to be important for its function: dimerization domain (DD), the *Ldb1*/Chip conserved domain (LLCD) and the LIM-interaction domain (LID) in the C-terminal part of the protein (top panel). HEK293T cells were transfected with constant amounts of *Isl1* (10 μ g) and GFP (1 μ g, used as a control of transfection efficiency) expression plasmids and increasing amounts of *Ldb1*, *Ldb1* Δ LID and DN-*Ldb1* (5 and 9 μ g). Immunoblot analysis of equal amounts of total protein extracts was performed using either anti-*Isl1* or anti-GFP antibodies. **(H)** Western blot analysis of whole cell lysates from HEK293T cells transfected with *Isl1*, *Isl1* Δ LIM1, *Isl1* Δ LIM2 and *Isl1*HOMEO alone or together with DN-*Ldb1* and GFP (internal control) using anti-*Isl1*, anti-FLAG and anti-GFP antibodies. **(I)** FLAG-HA-*Ldb1* and *Isl1* or *Isl1* deletion constructs were transiently expressed in HEK293T cells and immunoprecipitation with an anti-*Isl1* antibody was followed by immunoblot analysis with an anti-FLAG antibody.

Figure 3. *Ldb1* and *Isl1* interact to regulate heart development. **(A)** Co-immunoprecipitation of nuclear extracts from d5 EBs using anti-*Ldb1* antibody and detected with anti-*Isl1* antibody. **(B)** Percentage of beating d7 EBs derived from ES cells overexpressing either GFP alone (control) or together with *Isl1*, *Ldb1* or in combination. **(C-E)** Relative mRNA expression of cardiomyocyte (*Mlc2a*, *Mlc2v*) **(C)**, endothelial (*Flk1*, *VE-Cad*) **(D)** and smooth muscle (*SM-actin*, *SM-Mhc*) marker genes **(E)** in d7 EBs differentiated from ES cells overexpressing either GFP alone (control) or together with *Isl1*, *Ldb1* or *Ldb1*+*Isl1*. **(F, G)** Relative mRNA expression of cardiac progenitor marker genes in d4 EBs **(F)** and *Flk1* and *Pdgfr- α* in d3.75 EBs **(G)**

differentiated from ES cells overexpressing either GFP alone or together with *Isl1*, *Ldb1* or *Ldb1+Isl1*. For qPCR analysis of endogenous *Isl1* levels, primers located in the 5'UTR were utilized. Error bars represent SEMs derived from three biological replicates. **(H-J)** H&E staining of representative paraffin sections of E16.5 hearts of wild-type and *Isl1+/-Ldb1+/-* embryos (**H**, top panels), higher magnification of right and left ventricles showing thinner compact myocardium of the right ventricle in *Isl1+/-Ldb1+/-* embryos (**H**, bottom panels), DORV (**I**) or OA in E18.5 hearts (**J**) with VSD (**I, J**). Abbreviations: Ao, Aorta; LA, left atrium; LV, left ventricle; RA, right atrium; RV, right ventricle; DORV, double outlet right ventricle; OA, overriding aorta; VSD, ventricular septal defect. **(K)** Morphometric analysis of right ventricle compact myocardial thickness (n=4). **(L)** Relative mRNA expression analysis of cardiac progenitor and cardiomyocyte genes in dissected hearts and SHF of E9.25 wild-type, *Isl1+/-*, *Ldb1+/-* (controls) and double heterozygous *Isl1+/-Ldb1+/-* embryos. Data are mean \pm SEMs, n=4 for each genotype. * $p \leq 0.05$, ** $p \leq 0.01$, *** $p \leq 0.005$. See also Figure S2.

Figure 4. The dimerization domain of Ldb1 is required for cardiomyocyte differentiation.

(A) Confocal images of control and DN-Ldb1 overexpressing *Tg(myf7:EGFP-HsHRAS)^{s883}* zebrafish embryos stained with anti-GFP and anti-*Isl1* (red) antibodies at 48 hours post fertilization (hpf), showing shortened atrium and significant reduction of *Isl1+* cardiomyocytes at the venous pole. Arrows indicate *Isl1+* cells outside of the heart, which do not express the cardiomyocyte marker *myf7*. Scale bars, 50 μ m. **(B, C)** In situ hybridization of control, DN-Ldb1 overexpressing and *Isl1* mutant embryos at 48 hpf with *bmp4* (**B**) and *mef2cb* (**C**) probes. The arrows indicates *bmp4* expression at the sinus venosus. **(D)** Confocal images of control and DN-Ldb1 overexpressing embryos stained with anti-*Isl1* antibody (leftmost panels) and *in situ* hybridization of control and DN-Ldb1 overexpressing embryos at 10-15s stages with *isl1*, *nkx2.5*, *hand2*, *tbx5a* and *mef2cb* probes. **(E)** Percentage of beating d7 EBs derived from *Ldb1-/-* ES cells overexpressing either GFP alone (control) or together with *Isl1*, *Ldb1*, DN-Ldb1 or in

different combinations. **(F, G)** Relative mRNA expression analysis of cardiomyocyte **(F)**, smooth muscle and endothelial marker genes **(G)** in d7 EBs. **(H)** FACS analysis of Flk-1 and Pdgfr- α expression in d3.75 EBs. **(I)** Western blot analysis of total protein extracts of d5 EBs. **(J)** Relative mRNA expression of *Mef2c* and *Hand2* in d4 EBs. Error bars represent SEMs derived from three biological replicates. **(K, L)** ChIP of nuclear extracts from d5 EBs **(K)** and pools of dissected SHF from E8-E9 embryos (n=3) **(L)** using anti-Is11 and anti-Ldb1 antibodies or IgG as control. PCRs were performed using primers flanking conserved Is11 binding sites in the *Mef2c* promoter and the AHF enhancer. Fold enrichment values for EBs were calculated relative to IgG control and for embryos relative to a genomic region which does not contain conserved Is11 binding sites. **(M, N)** ChIP of nuclear extracts from d5 EBs **(M)** and pools of dissected SHF from E8-E9 embryos **(N)** using anti-Is11 and anti-Ldb1 antibodies or IgG as a control. PCRs were performed using primers flanking conserved Is11 binding sites in the *Hand2* promoter and the OFTRV enhancer (McFadden et al., 2000). See also Figures S3-S7.

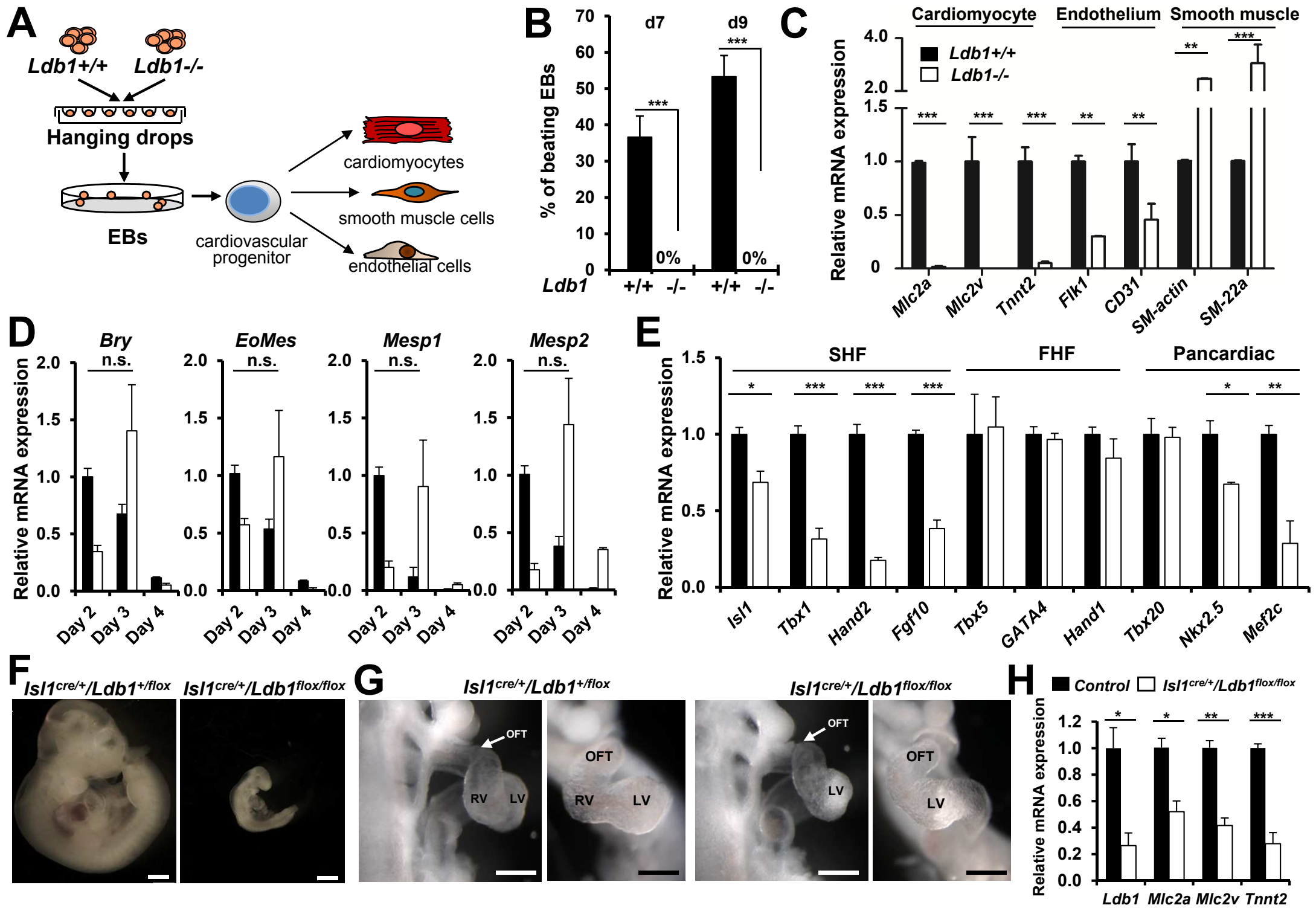
Figure 5. Ldb1 facilitates long range enhancer-promoter interactions within the *Hand2* and *Mef2c* loci. **(A)** Schematic representation of the *Hand2* genomic locus and the position of the DpnII restriction sites, used in the 3C assay (top). 3C-qPCR relative crosslinking frequency observed in WT, *Ldb1*^{-/-} ES cells and d5 EBs derived from *Ldb1*^{-/-} ES cells overexpressing either GFP alone or together with Is11, Ldb1, DN-Ldb1 or in different combinations. The *Hand2* promoter was used as viewpoint to the *Hand2* OFTRV enhancer or to negative control regions downstream of the *Hand2* promoter, between the *Hand2* promoter and the OFTRV enhancer and upstream of the OFTRV enhancer. Values were normalized to the *β -actin* locus and the highest value for the OFTRV enhancer in d5 WT EBs was set as one. Data are mean \pm SEMs, n=3. **(B)** Schematic representation of the *Mef2c* genomic locus and the position of the restriction sites of *HindIII*, used in the 3C assay (top). 3C-Seq analysis of *Mef2c* AHF- (middle panel) and *Mef2c* promoter-associated regions (bottom panel) in d5 wild-type and *Ldb1*^{-/-} EBs. The

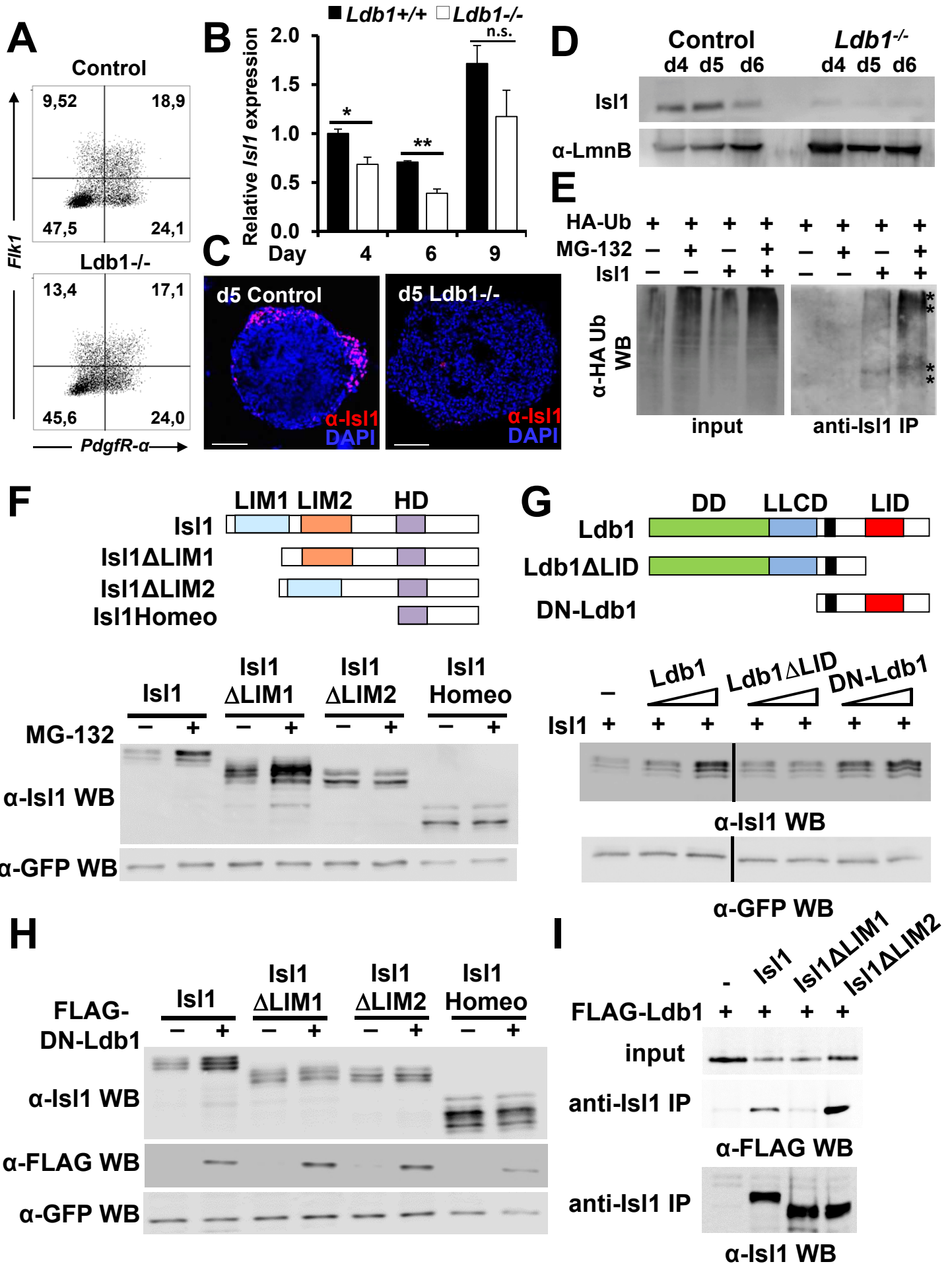
viewpoint is indicated with an eye symbol. **(C)** 3C-qPCR relative crosslinking frequency observed in EBs at different days (top panels) and in microdissected SHF region, brain or tail from pools of embryos at different developmental stages (bottom panel). Data are mean \pm SEMs, n=3. **(D)** 3C-qPCR relative crosslinking frequency observed in d4 (top) and d5 (bottom) EBs derived from WT and *Ldb1*^{-/-} ES cells or *Ldb1*^{-/-} ES cells overexpressing either GFP alone or together with *Isl1*, *Ldb1*, DN-*Ldb1* in different combinations. Data are mean \pm SEMs, n=3. For the 3C-qPCR in **C** and **D** the HindIII fragment containing the *Mef2c*-AHF was used as viewpoint (red bar, eye symbol). **(E)** Schematic representation of alternative *Mef2c* transcripts (top) and absolute quantification of these transcripts using primers indicated in the scheme (bottom). **(F)** ChIP of d4 EBs derived from WT and *Ldb1*^{-/-} ES cells using antibodies against H3, H3k4me1, H3K27Ac, p300, RNA-PolIIIS5p and IgG as a control. (*p \leq 0.05, **p \leq 0.01, ***p \leq 0.005). See also Figure S7.

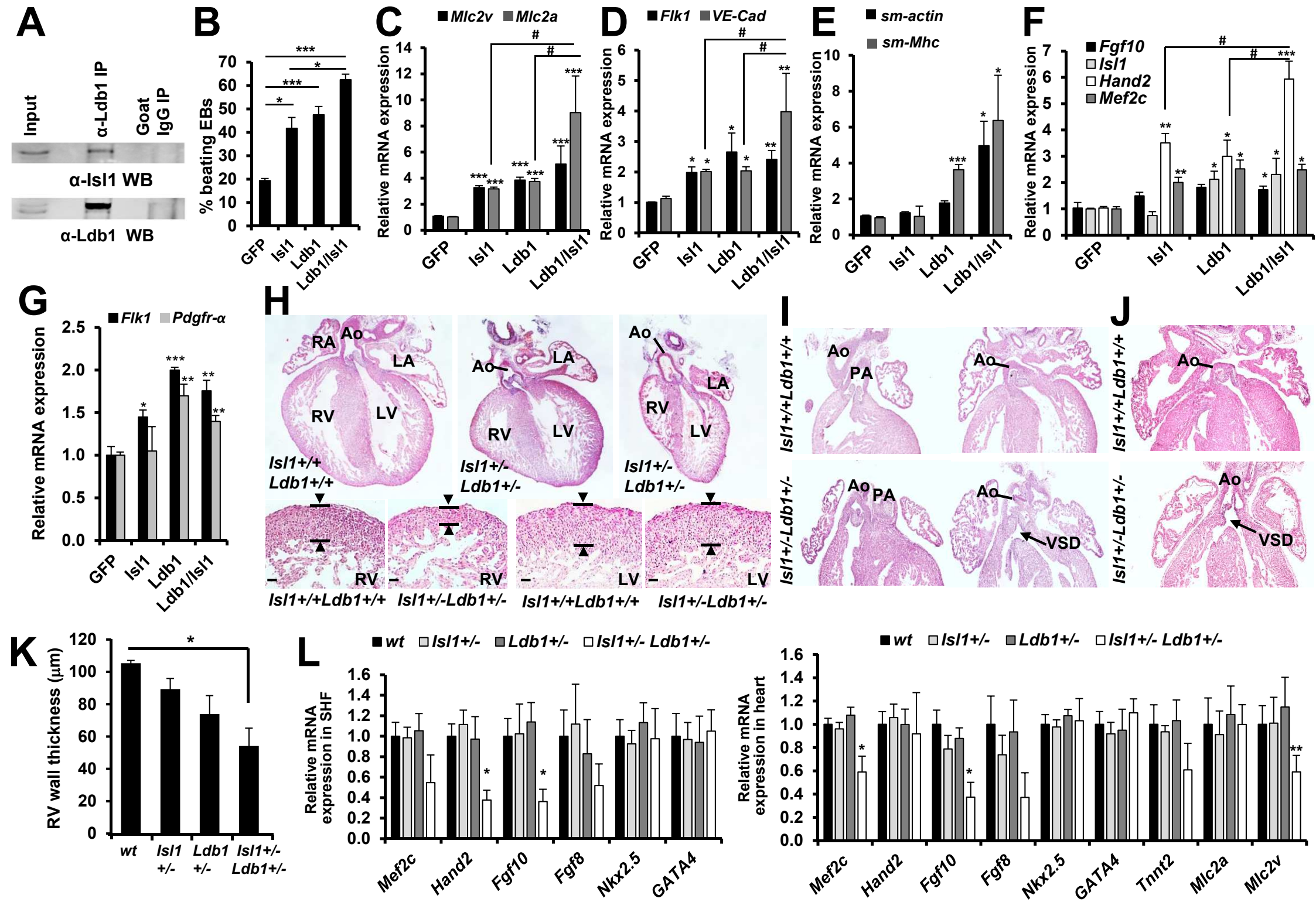
Figure 6. *Ldb1* promotes chromatin looping events between the AHF enhancer and genes which play key roles in cardiovascular development. **(A, B)** Gene ontology analysis of genes interacting with the *Mef2c* AHF **(A)** or the *Mef2c* promoter **(B)**, overrepresented in wild-type versus *Ldb1*^{-/-} cells. **(C)** Schematic representation of 3C-seq results showing specific interactions of the *Mef2c* AHF (located at chromosome 13 (Chr13)) with cardiac specific genes on Chr13 or on other chromosomes. The HindIII restriction sites are shown as black bars. Y axes - reads per million. **(D, E)** 3C-qPCR validation of the interactions observed using the 3C-seq approach in WT or *Ldb1*^{-/-} d5 EBs **(D)** or in microdissected SHF regions and tails of E8-9 embryos **(E)** using the *Mef2c*-AHF as viewpoint. Data are mean \pm SEMs, n=3. (*p \leq 0.05, **p \leq 0.01, ***p \leq 0.005). See also Figure S7.

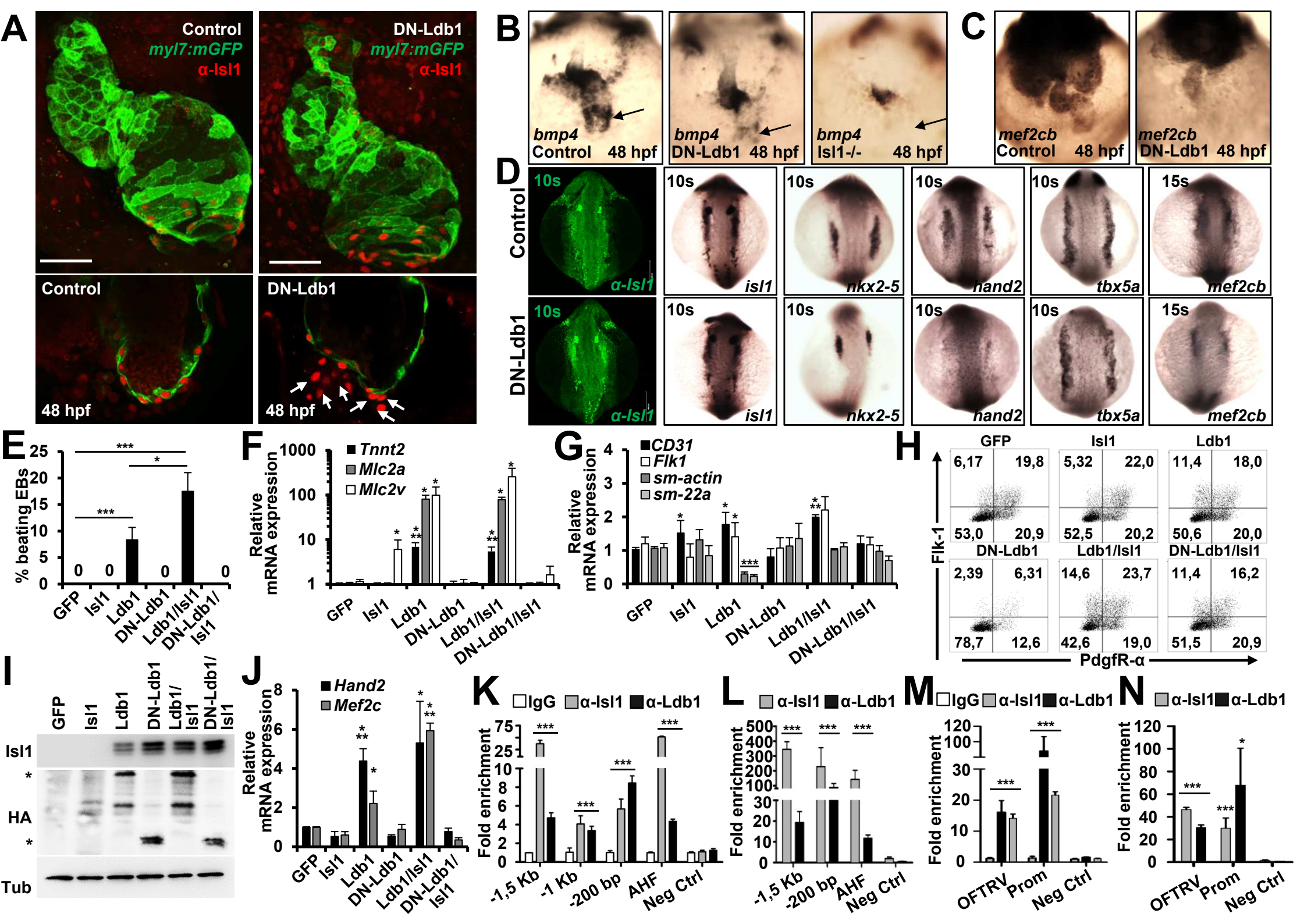
Figure 7. The *Isl1/Ldb1* complex orchestrates a network for transcriptional regulation and coordination in three-dimensional space during cardiogenesis. **(A)** Relative mRNA

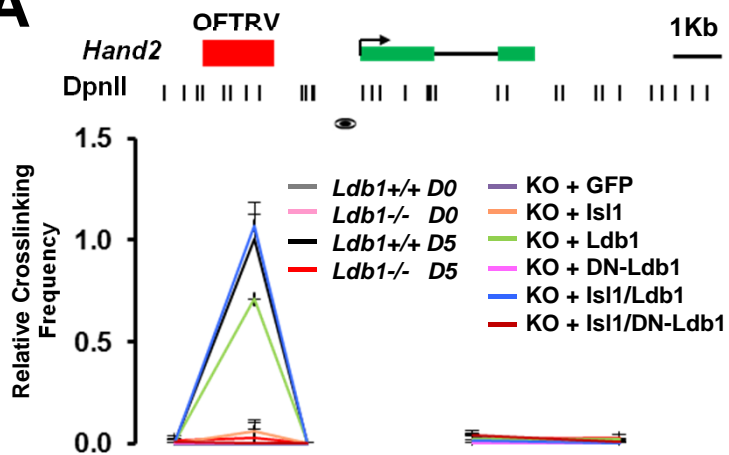
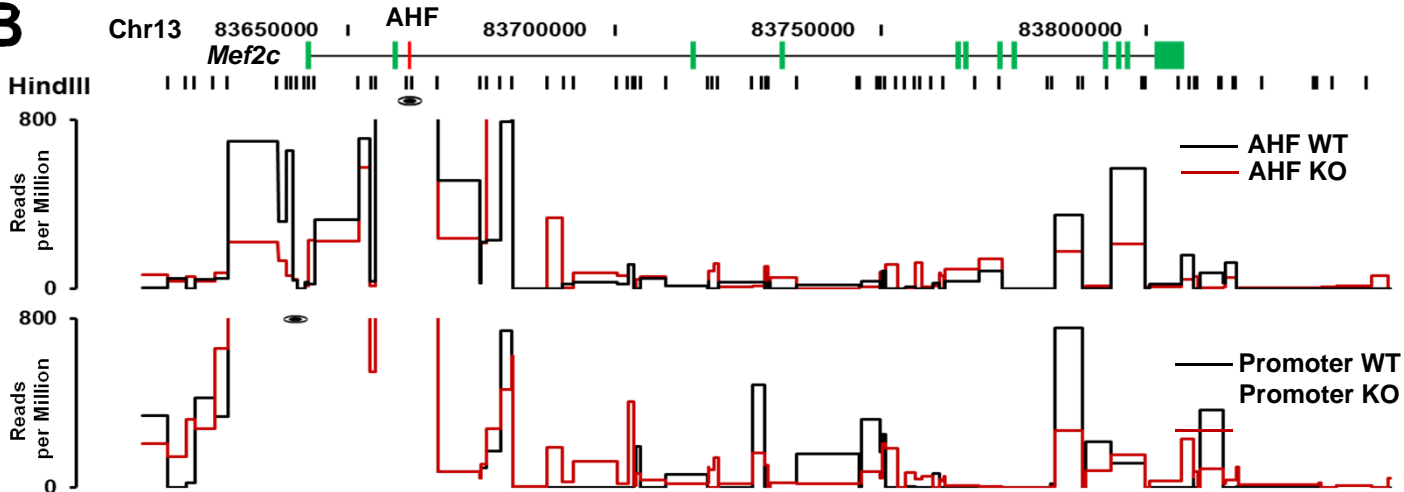
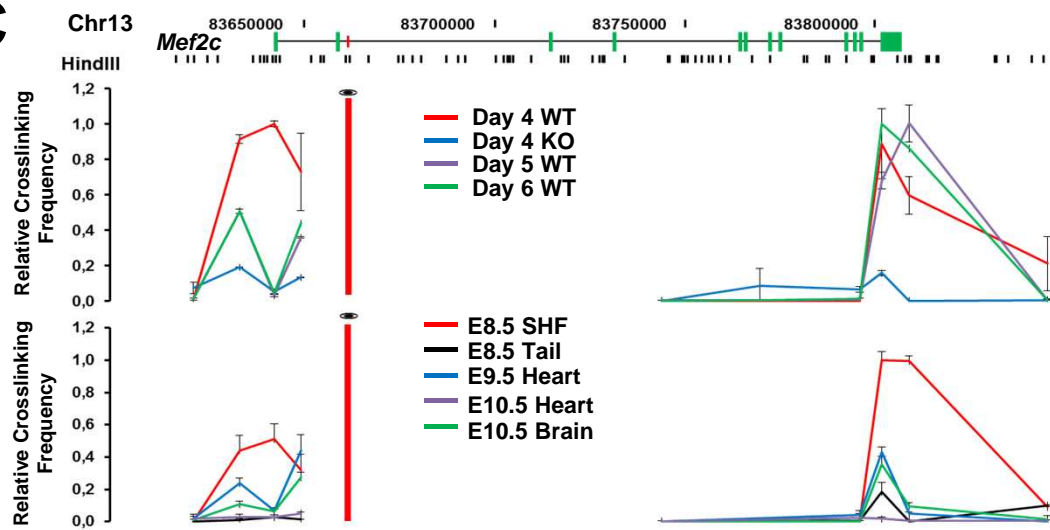
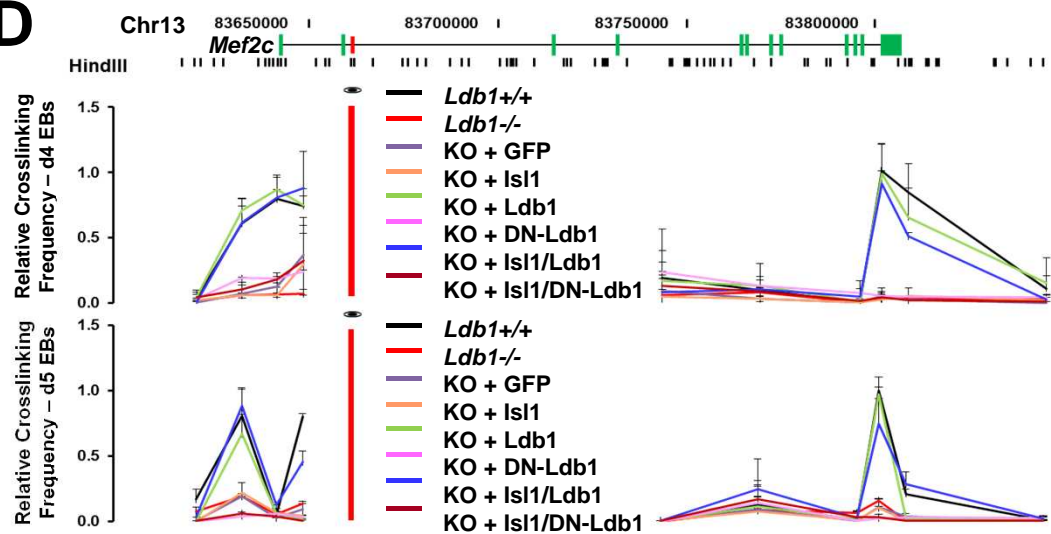
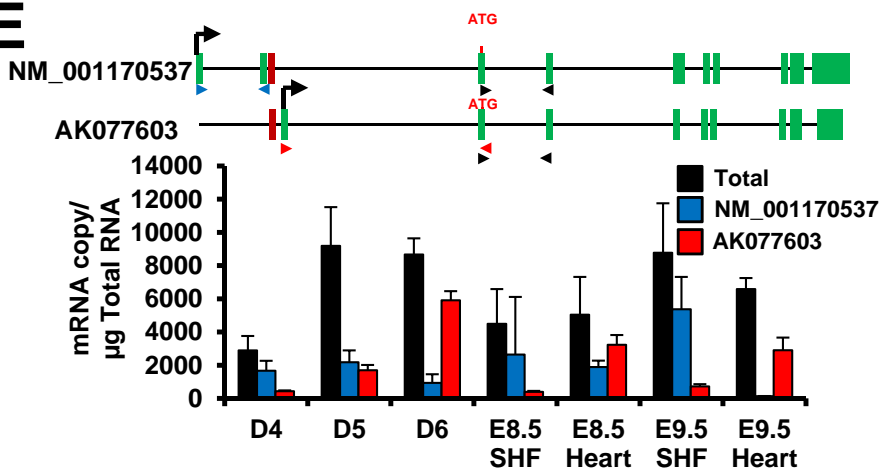
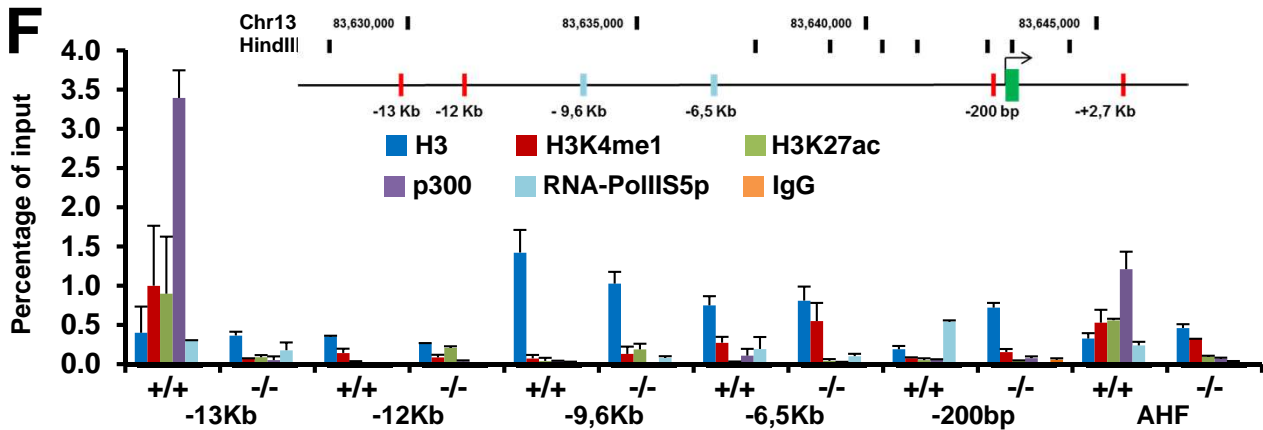
expression analysis in d4 and d6 WT and *Ldb1*^{-/-} EBs of selected genes identified in the 3C-seq analysis to specifically interact with the *Mef2c*-AHF in WT but not in *Ldb1*^{-/-} EBs. **(B)** Relative mRNA expression analysis of selected genes in d5 EBs overexpressing either GFP alone (control) or together with *Isl1*, *Ldb1*, DN-*Ldb1* or in different combinations. **(C-D)** Relative mRNA expression analysis of selected genes in microdissected SHF **(C)** or heart **(D)** of WT or *Isl1*^{+/-} *Ldb1*^{+/-} E9.25 embryos. Data are shown as mean ± SEMs, n=4. (*p≤0.05, **p≤0.01, ***p≤0.005). **(E)** Model of the role of *Ldb1* in heart development. *Ldb1* binds to *Isl1* and protects it from proteasomal degradation. The stabilized *Isl1*/*Ldb1* complex orchestrates a network for transcriptional regulation and coordination in three-dimensional space during cardiac progenitor cell differentiation and heart development.





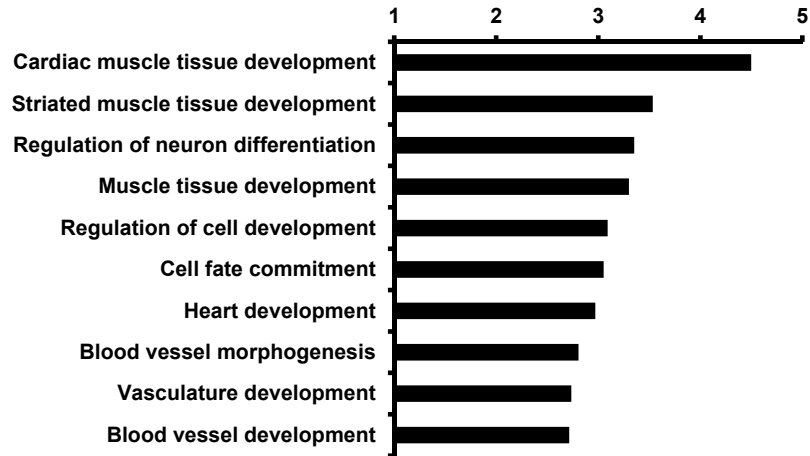




A**B****C****D****E****F**

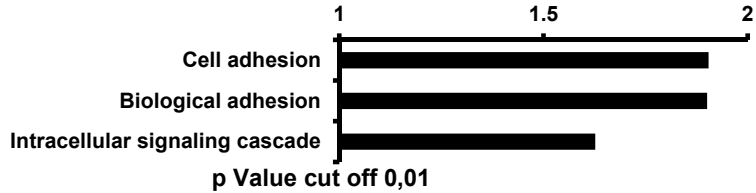
A

Ratio of overrepresentation WT/KO
Viewpoint AHF

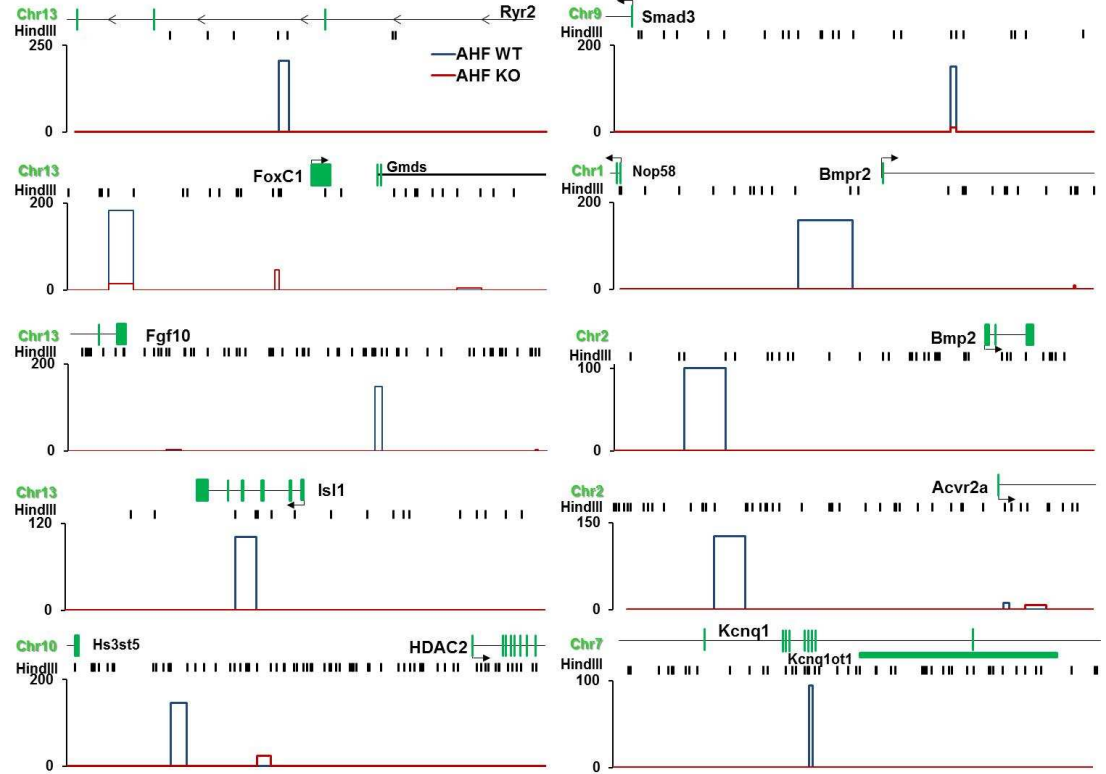


B

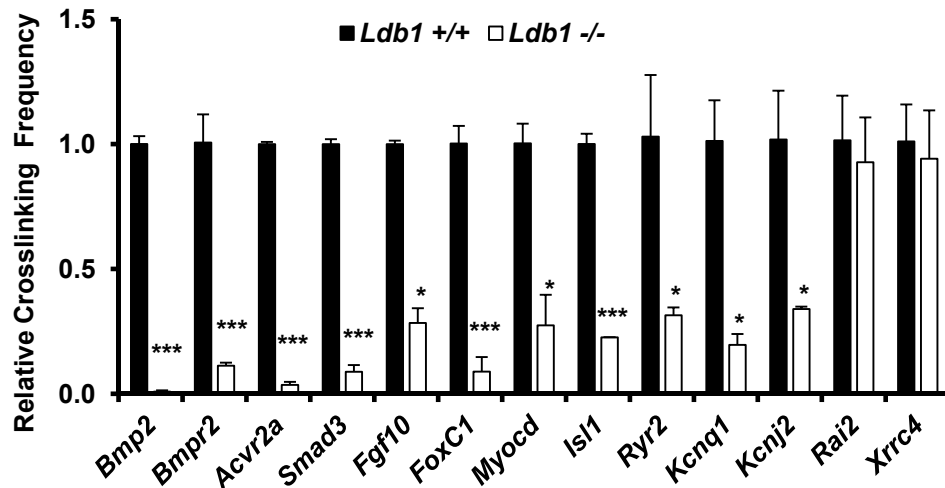
Ratio of overrepresentation WT/KO
Viewpoint *Mef2c* Promoter



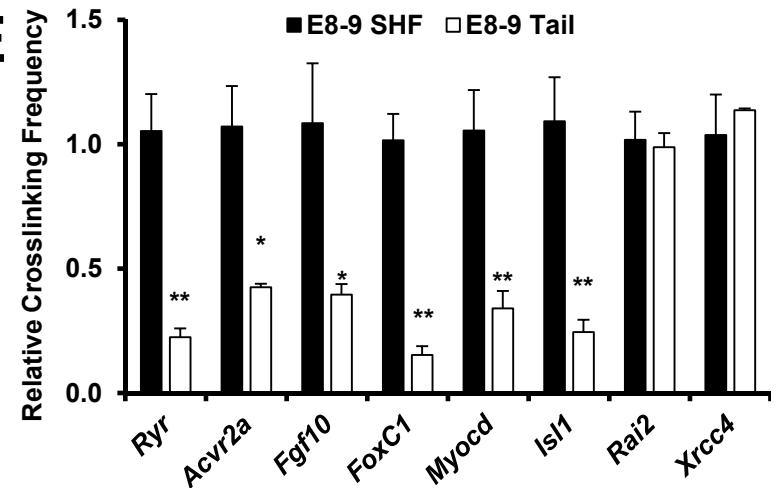
C

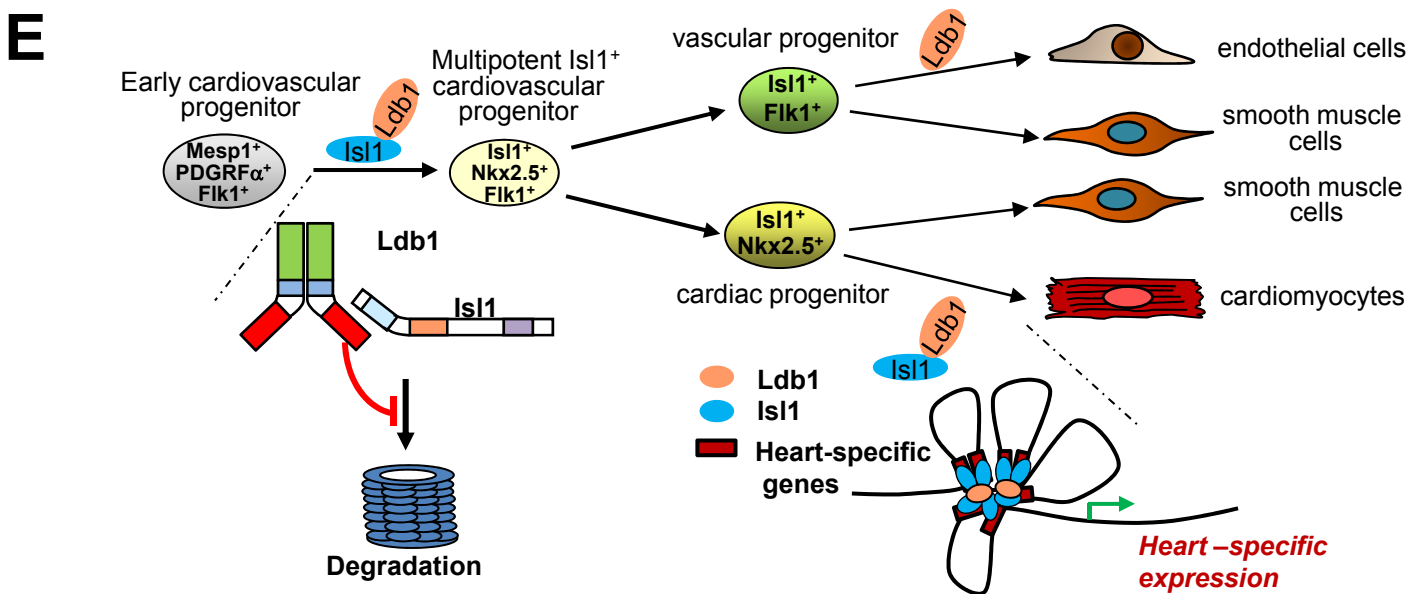
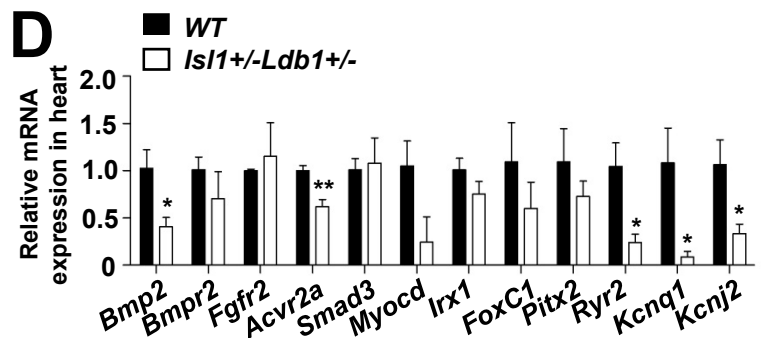
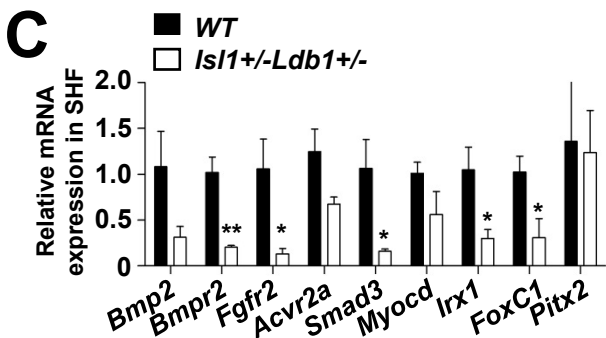
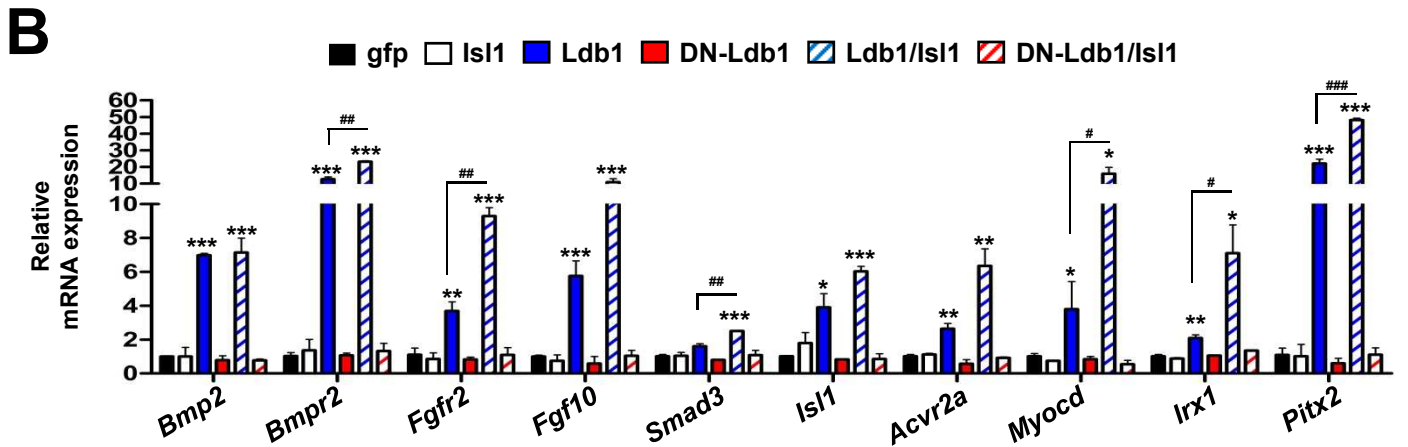
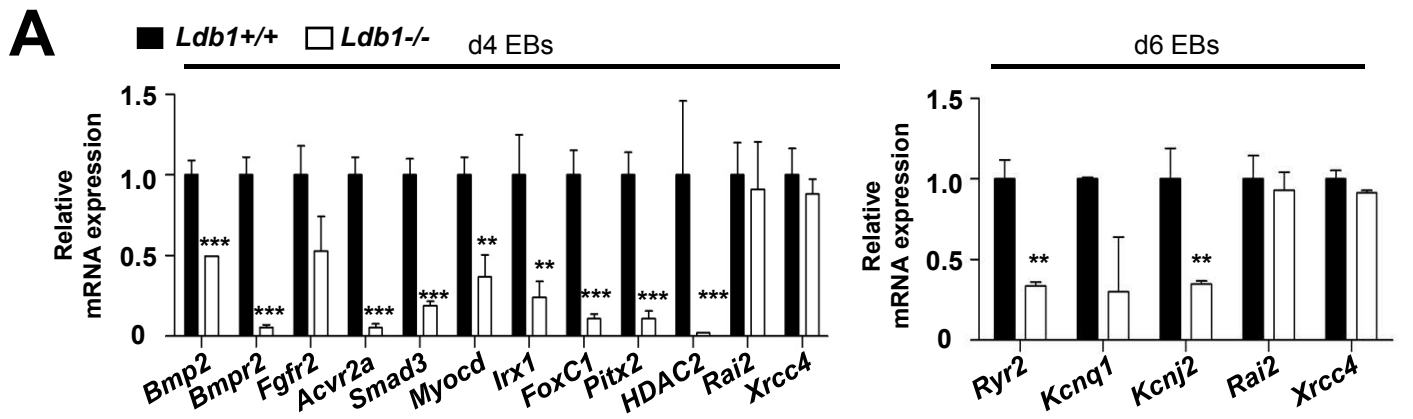


D



E





SUPPLEMENTAL FIGURES:

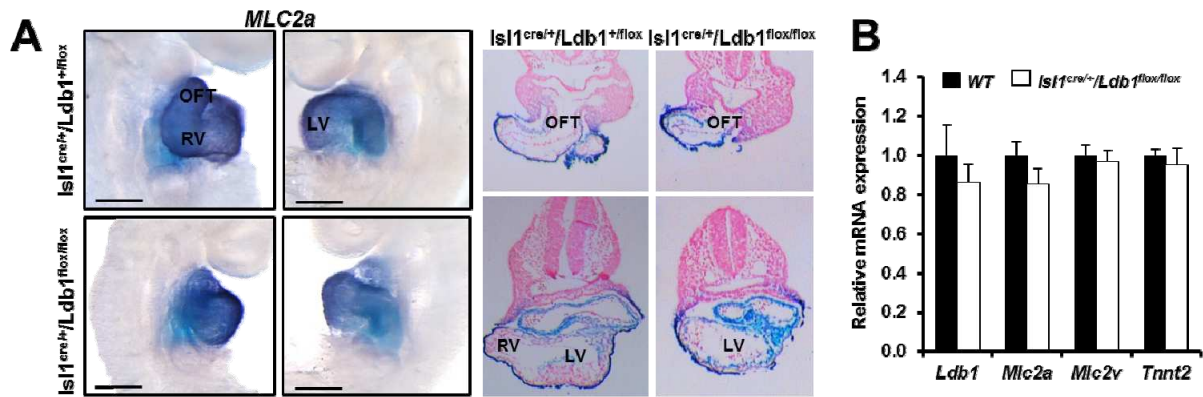


Figure S1, related to Figure 1. Aberrant cardiac morphology in *Isl1*^{cre/+}/*Ldb1*^{flox/flox} embryos.

(A) Left and right views of E9.5 control and *Isl1*^{cre/+}/*Ldb1*^{flox/flox} embryos after in situ hybridization with an *Mlc2a* riboprobe and corresponding sections, demonstrating aberrant cardiac morphology. Scale bars, 500 μ m. Abbreviations: OFT, outflow tract; RV, right ventricle; LV, left ventricle. **(B)** Relative mRNA expression analysis of cardiomyocyte genes in dissected left ventricles of E9.25 control and *Isl1*^{cre/+}/*Ldb1*^{flox/flox} embryos. Data are mean \pm SEMs, n=3 for each genotype.

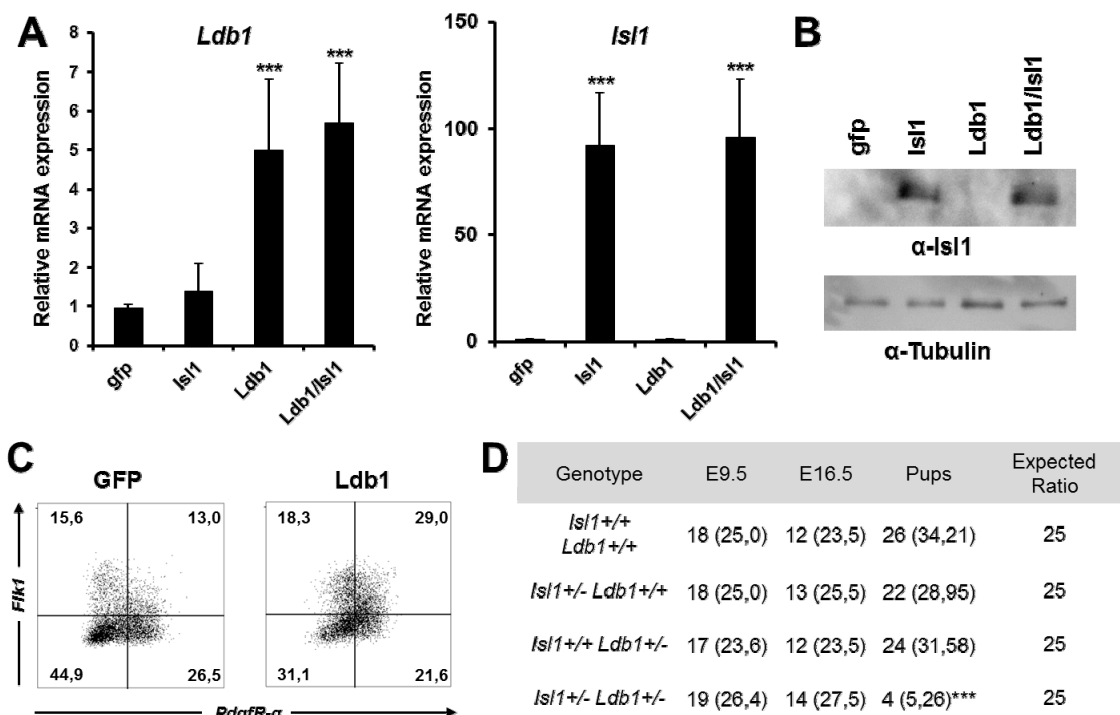


Figure S2, related to Figure 3. *Ldb1* and *Isl1* interact to regulate heart development. (A) Relative mRNA expression of *Ldb1* and *Isl1* in ES cells overexpressing either GFP alone (control) or together with *Isl1*, *Ldb1* or a combination of *Isl1/Ldb1*. **(B)** Western blot analysis of total protein extracts of ES cells overexpressing either GFP alone (control) or together with *Isl1*, *Ldb1* or *Ldb1+Isl1*, using *Isl1* antibody. Tubulin served as loading control. **(C)** FACS analysis of *Flk-1* and *PdgfR- α* expression in d3.75 EBs differentiated from ES cells overexpressing either GFP alone (control) or together with *Ldb1*. **(D)** Analysis of the genotype of animals born from the cross *Isl1*^{+/-} x *Ldb1*^{+/-}. Total numbers (percentage) of recovered embryos or pups for all four different genotypes are shown. ***p<0,0001 Chi squared test.

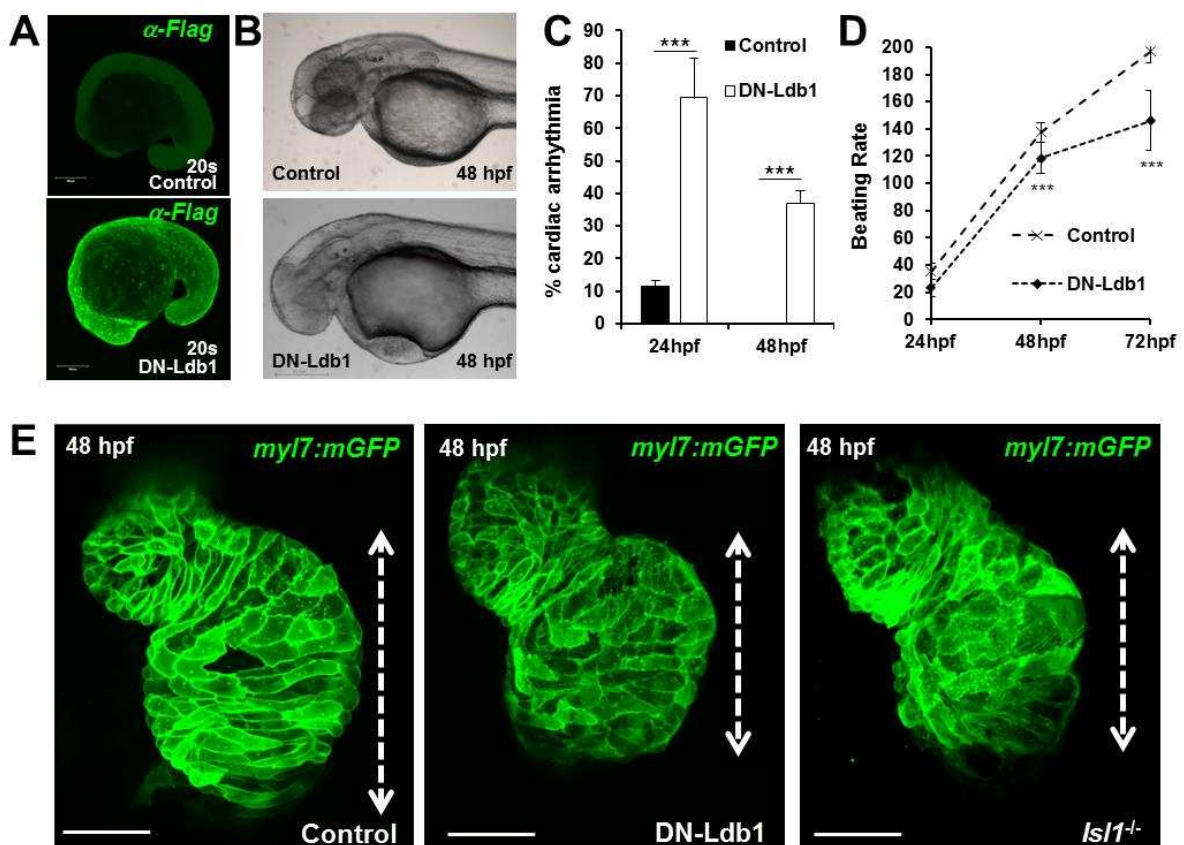


Figure S3, related to Figure 4. Cardiac morphogenesis defects in zebrafish embryos overexpressing DN-Ldb1. (A) Confocal images of control and *FLAG-HA-DN-Ldb1* mRNA injected zebrafish embryos, stained with anti-FLAG antibody at 20 somites. **(B)** Control or *DN-*

Ldb1 mRNA injected *Tg(myI7:EGFP-HsHRAS)^{s883}* embryos at 48 hpf. Lateral view, anterior to the left. **(C-D)** Percentage of embryos with cardiac arrhythmia **(C)** and analysis of the number of heart beats per minute **(D)** measured at 24, 48 and 72 hpf in control and DN-*Ldb1* overexpressing zebrafish embryos. **(E)** Confocal images of control, DN-*Ldb1* overexpressing and *Isl1* mutant *Tg(myI7:EGFP-HsHRAS)^{s883}* hearts, showing shortening of the atrium (dotted lines) in DN-*Ldb1* overexpressing and *Isl1* mutant embryos.

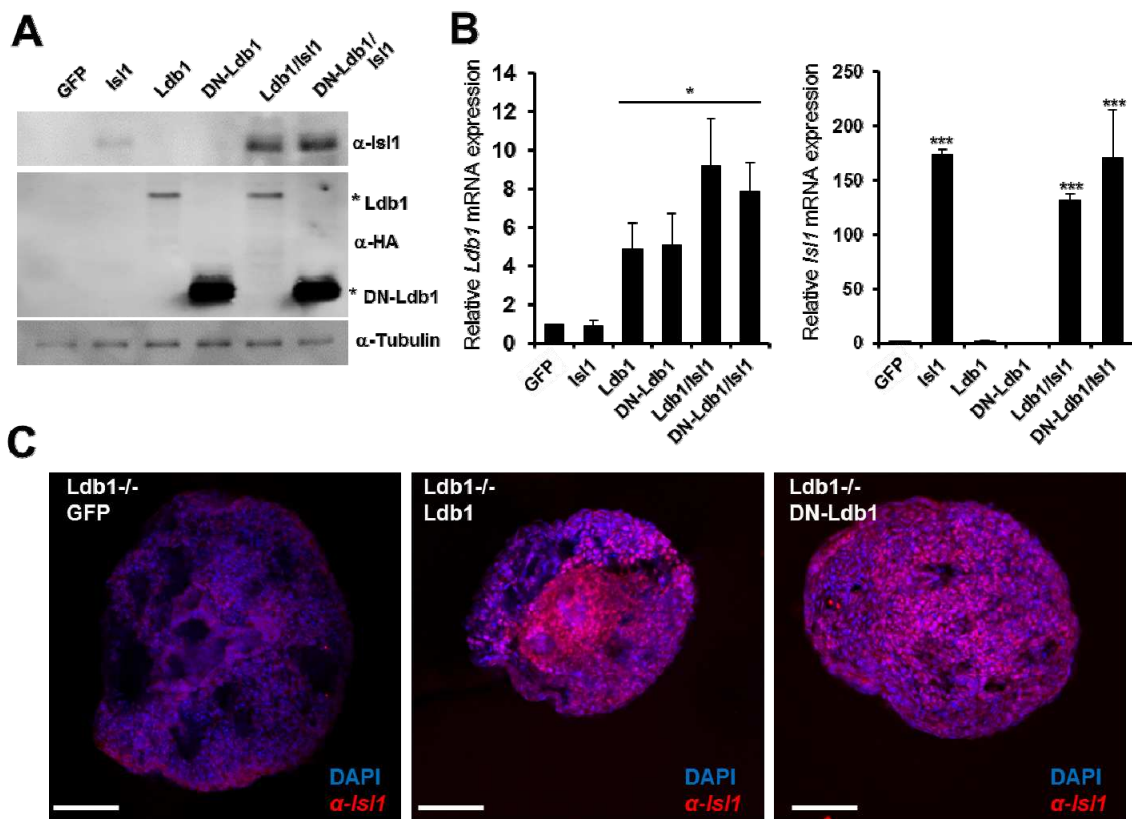


Figure S4, related to Figure 4. Overexpression of *Ldb1* and DN-*Ldb1* restores *Isl1*+ cells.

(A) Western blot analysis of total protein extracts of *Ldb1*^{-/-} ES cells overexpressing either GFP alone (control) or together with *Isl1*, *Ldb1*, DN-*Ldb1* or in different combinations. **(B)** Relative mRNA expression of *Ldb1* and *Isl1* in *Ldb1*^{-/-} ES cells overexpressing GFP, *Isl1*, *Ldb1*, DN-*Ldb1* or in different combinations. **(C)** *Isl1* immunostaining on vibratome sections of d5 EBs differentiated from *Ldb1*^{-/-} ES cells overexpressing either GFP alone (control) or together with *Ldb1* and DN-*Ldb1*. Scale bars, 100 μm.


```

mouse  TATGAAAGCAATTTTCATTTTTTAGGAATGATTTT---GGATAGACTTC CGATTGGATATTTTCCATTGGAAC TAACAGTGTAGAGGCTTG
human  TATGAAAGCAATTTTCATTTTTTAGGAATGATTTTTCATGGATAGACTTC CGATTGGATATTTTCCATTGGAAC TAGCAGCATAGGGGGTGC

mouse  GGGTGGGGAGAG-----AGCAGTTCGTGTTCTTTTGCCAGCACTGACAAAAGGTCGGTTGTCAATGATACCTTTACAGCTAAATT
human  GGGGGGGGGAGGTCGGAGGGAAGCAATTCGTGTTCTTTTGCCAGCACTGACAAAAGGTCGGTTGTCAAGTGTACCTTTACAGCTAAATT

mouse  TACTCCAGAGTGCATGAAACAGGTGCACCCCTGGCCCTGCCAGACACTTGTGCAGAGGGGATCAGCCTCTCACCGCTTGACGATCAAGGGGG
human  TACTCCAGAGTGCACAGAAACAGGTGCACCTCGGCCCTGCCAGACACTTGTGCAGAGAGATCACGCTCTCACGGCTTGACGATCAAGGGGG
          HindIII
mouse  CAAAGCTTCGGTGTTCATAGAAAAGGAGAGGAGGGCGAGCGCAGCCAAACTGGGGGGTTT
human  CAAAGCCTCGGTCTTCATAGAAAAGGAGAGGAGGCAACGCAGCCAAACTGGGGGGTTT
  
```

Mef2c -13Kb

Mouse mm9 chr13 83629799-83630029
 Human hg19 chr5 88214651-88214411

```

mouse  TATTTGAGAGGGTGGTATCAATTAACATATATTTATCTATAAACCATCTTGCAATTACTACCACCTTCACAAATTTATCATTAAACACATTTG
human  TGCTTGAGAGGGTGGTATCAATTAACATATATTTATCTATAAAGCCATCTTGCAATTACTACCACCTTCACAAATTTATCATTAAATGCATTTG

mouse  GCAGATTTTTTTTG---CAAAGTAACTTTATTTAAAGGTTAATCAAAAATCTTAGAATAGCAATTTATTA TAATGTGATTTT TGATAAATG
human  GCAGATTTTTTTTCTCCAAAGTAACTTTATTTAAAGGTTAATCAAAAATCTTAGAATAGCAATTTATTA TAATGTGATTTT TGATAAATG

mouse  ACTAAATCAGTGGCTCTTAAABACACCCTTGTCTCAGTCCTGCTCAGTATACACCCACACT
human  ACTAAATCAGTGGCTCTTAAAGAACACCCTTGTCTCAGTCCCACCTCAGTATACACCCACAGT
  
```

Mef2c -12Kb

Mouse mm9 chr13 83631203-83631643
 Human hg19 chr5 88213106-88212651

```

mouse  AGGCATBACCATCTTGCTTTAATGAGCATTACTAABCTACACTCGACTTTATCCAG----TGGABGGCTAABAGCABAGGA--CBGTCTT
human  AGGTACATACATGTGCATTTAATGAACGTTACTGACTACACTTTACACCATGCAAGGCACATAAAGGGAGGAGGACAGCCAAACAGTCTC

mouse  GGCCCTTGGCAAGGATGTAAGAA-----TATCAGTGCATGTATGTCAABCAABCACTCAGGACATCA-TGAAAGCACTCAATCCACT
human  AGTTCTCAACAAGAGCTAABAAAGABATTAACAAGTAACTGCATGCCAAGCACAAGTCAATGATATCACTGAAAATTAACAACCTGAT

mouse  TCCCATTGGAAACCGCAAGGGAAAGTCTTCAAGGTCATGG-----AGAAAGTAGGTGTTATT-AGGACACCTCAAGA-----TCTC
human  TCCCTTTGAAAGCCTCAGGAAGAAAGCGGTGAATCATGGAAGTCTTAAGGAGTAGGTGCCATTAAAATAGTTCAAGAGAAATTTCCC

mouse  TGCAGMTAGCATGTACTAGTGCCTTTACTAACA-----CCA-----CCACAGTAAATTTCTTGCTCTCTG
human  T---GATTACATAAATAGTGAATTCCTACTAGTGCATGAAAGCATTGAAAGTAAAGGTCACAGGTTTTCAGAGTAAATTCCTCCTTTCTT

mouse  GGGGACATTAAGTCCATTTGT---TTTCATCAAATTACCTTTGGGGATAC---AAATGATAAATG GTGATTTAATAGCCA CCCAGTAGA
human  ABAACAG-CAATCTGTTTTCATCTCATCAAGTTA-GTTTGGTGCATAAAABAAATGATAAATG CTGAATTAATGGCCATTCAGTATG

mouse  AGGAACAAGGAAATTTCTCTTTTCATGGT
human  AAGAACAAGGAAATTTCTCTTTTCAGGT
  
```

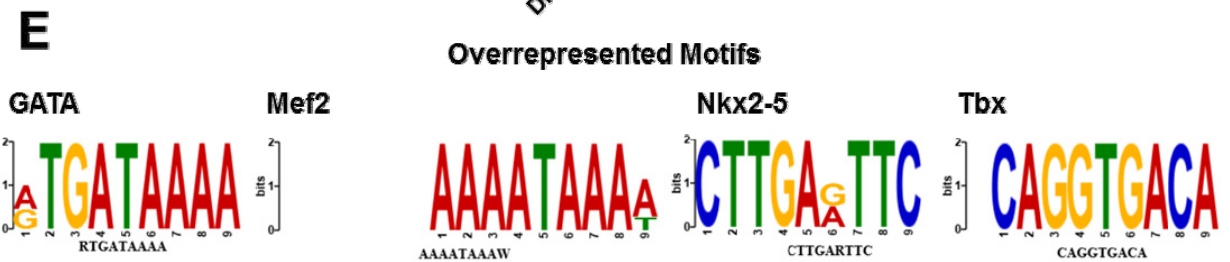
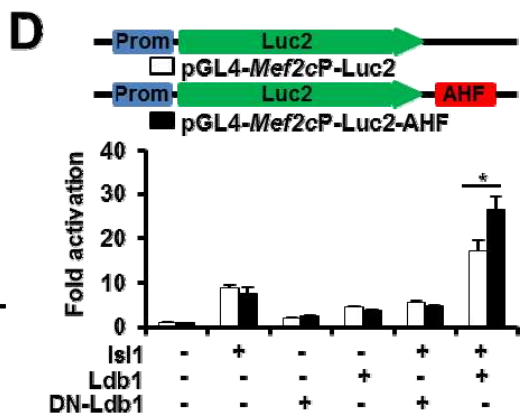
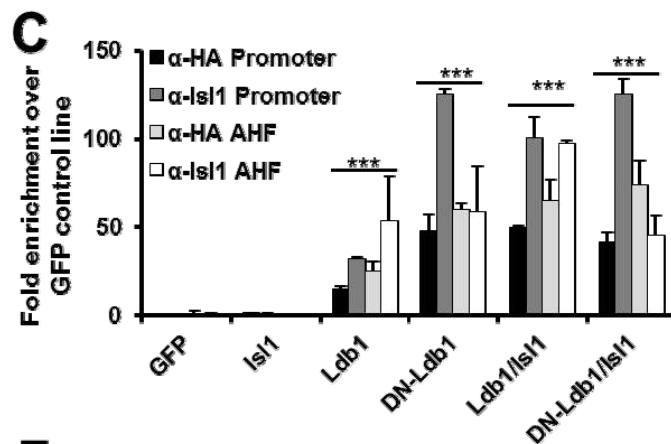
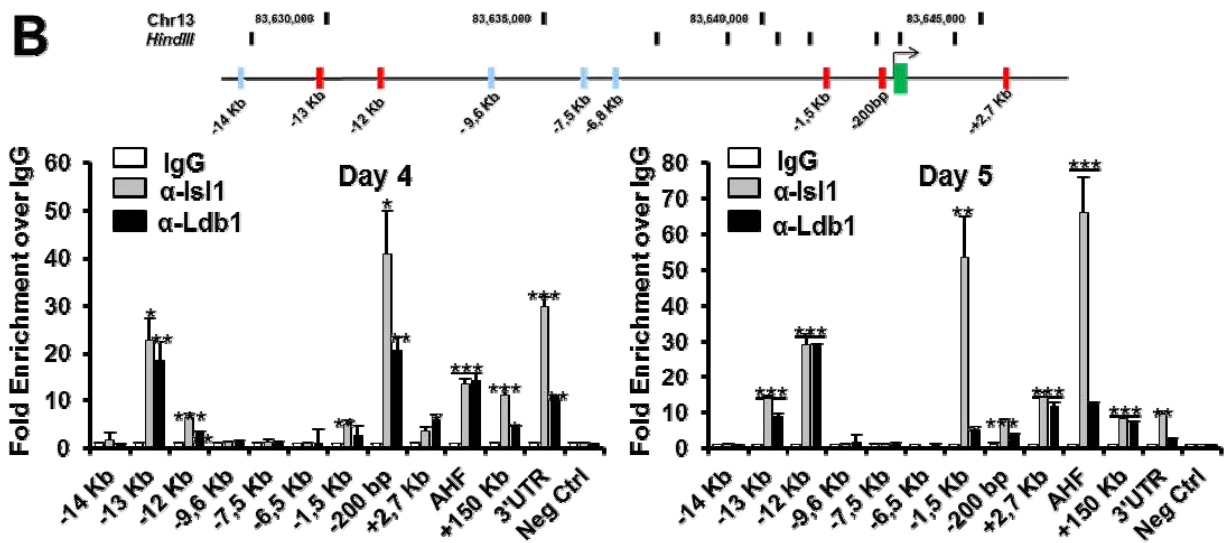
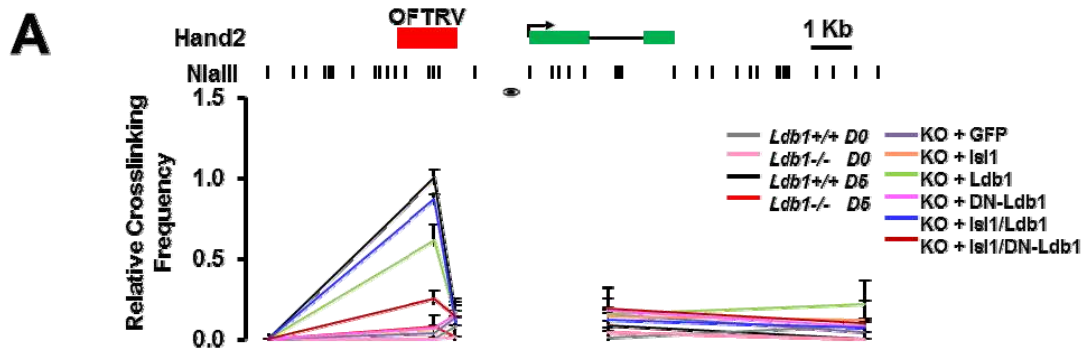



Figure S7, related to Figure 5 and Figure 6. Ldb1 promotes chromatin looping events between the AHF enhancer and genes which play key roles in cardiovascular development. **(A)** Schematic representation of the *Hand2* genomic locus and the position of the *Nla*III restriction sites, used in the 3C assay (top). 3C-qPCR analysis of WT, *Ldb1*^{-/-} ES cells and d5 EBs derived from WT and *Ldb1*^{-/-} ES cells or *Ldb1*^{-/-} ES cells overexpressing either GFP alone (control) or together with *Isl1*, *Ldb1*, DN-*Ldb1*, or in different combinations (bottom). **(B)** ChIP of nuclear extracts from d4 (left) and d5 (right) EBs using anti-*Isl1* and anti-*Ldb1* antibodies or IgG as a control. PCRs were performed using primers flanking conserved *Isl1* binding sites (red) or not containing *Isl1* consensus sites (light blue) in the -14 to -5.5 kb region within the *Mef2c* locus found by the 3C-seq in close proximity to the *Mef2c*-AHF. **(C)** ChIP of FLAG-HA-*Ldb1* and FLAG-HA-DN-*Ldb1* or *Isl1* in nuclear extracts from d4 EBs using anti-HA and anti-*Isl1* antibodies. PCRs were performed using primers flanking the conserved *Isl1* binding sites in the *Mef2c* promoter and the AHF enhancer. Fold enrichment values were calculated relative to the GFP control. **(D)** COS7 cells were transiently transfected with a 100 ng luciferase reporter construct containing the *Mef2c* promoter alone or in combination with the AHF enhancer, located downstream of the luciferase gene (Dodou et al., 2004), together with pcDNA (400 ng), *Isl1* (400 ng), *Ldb1* (400 ng), DN-*Ldb1* (400 ng) or in combinations. The luciferase levels were normalized for the β -galactosidase activity of a cotransfected RSV-lacZ reporter (10 ng) and presented as fold activation relative to the luciferase levels of the reporter construct alone. All transfections were performed at least three times in triplicates, and representative experiments with the standard deviations are shown. See also Figure S3, S4 and S5. (* $p \leq 0.05$, ** $p \leq 0.01$, *** $p \leq 0.005$). **(F)** Motif enriched in the genomic regions found in close proximity to the *Mef2c* AHF in d5 EBs.

Table S1, Related to figure 6. Peak coordinates of sequences interacting with the *Mef2c*-AHF and the *Mef2c*-promoter in d5 EBs.

Table S2. Synthetic oligonucleotides used in the study.

Primers used for RT-PCR analysis:

Primer Name	Sequence 5'→3'	Accession Number
qGAPDH_for	AACTTTGGCATTGTGGAAGG	XM_001476707
qGAPDH_rev	GGATGCAGGGATGATGTTCT	
q5'UTRIsi1_for	ACAGCACCAGCATCCTCTCT	NM_021459
q5'UTRIsi1_rev	TCCCATCCCTAACAAAGCAC	
qIsi1_for	GCGACATAGATCAGCCTGCT	NM_021459
qIsi1_rev	GTGTATCTGGGAGCTGCGAG	
qLdb1_for	GGGGGGTGGCAACACCAACAACA	NM_001113408
qLdb1_rev	CCCCCACCACCATCACATCAGGT	
qNkx2.5_for	AAGCAACAGCGGTACCTGTC	NM_008700
qNkx2.5_rev	GCTGTCGCTTGCACTTGATAG	
qMef2c_for	TCCATCAGCCATTTCAACAA	NM_001170537
qMef2c_rev	AGTTACAGAGCCGAGGTGGA	
qTbx1_for	CGACAAGCTGAACTGACCA	NM_011532
qTbx1_rev	AATCGGGGCTGATATCTGTG	
qTbx20_for	GCAGCAGAGAACCACATCAA	NM_020496
qTbx20_rev	GTGAGCATCCAGACTCGTCA	
qTbx5_for	ATGGTCCGTAAGTGGCAAAG	NM_011537
qTbx5_rev	ACAAGTTGTCGCATCCAGTG	
qGATA4_for	TCTCACTATGGGCACAGCAG	NM_008092
qGATA4_rev	GCGATGTCTGAGTGACAGGA	
qHand1_for	GCGGAAAAGGGAGTTGCCTCAGC	NM_008213
qHand1_rev	GCTCCAGCGCCAGACTTGC	
qHand2_for	CGGAGAGGGCGAGGCCTTCA	NM_010402
qHand2_rev	CAGGGCCCAGACGTGCTGTG	
qMlc2v_for	CTGCCCTAGGACGAGTGAAC	NM_010861
qMlc2v_rev	CCTCTCTGCTTGTGTGGTCA	
qMlc2a_for	CCCATCAACTTCACCGTCTT	NM_022879
qMlc2a_rev	CGTGGGTGATGATGTAGCAG	
qTnnt2_for	ATCCCCGATGGAGAGAGAGT	NM_011619
qTnnt2_rev	CTGTTCTCCTCCTCCTCAGC	
qSM-actin_for	CTGACAGAGGCCACTGAA	NM_007392
qSM-actin_rev	AGAGGCATAGAGGGACAGCA	
qSM-22a_for	AACGACCAAGCCTTCTCGCC	NM_011526
qSM-22a_rev	TCGCTCCTCCAGCTCCTCGT	
qSM-mhc_for	AGGAAACACCAAGGTCAAGCA	NM_001161775
qSM-mhc_rev	AGCCTCGTTTTCTCTCTGTA	
qBry_for	AGGGAGACCCACCGAACGC	NM_009309
qBry_rev	CCGGGAACATCCTCCTGCCGT	
qEoMes_for	CAGGGCAGGCGCATGTTTCT	NM_010136
qEoMes_rev	TCCGCTTTGCCGAGGCTCAC	
qFlk1_for	GGTTTTGGTTTTGGAAGTT	NM_010612
qFlk1_rev	AGGAGCAAGCTGCATCATT	
qPDGFra_F	GGAACCTCAGAGAGAATCGGC	NM_001083316
qPDGFra_R	CATAGCTCCTGAGACCCGC	
qVE-Cad_for	TGAGGCAATCAACTGTGCTC	NM_009868
qVE-Cad_rev	TTCGTGGAGGAGCTGATCTT	
qlrx1_for	CTTCTCGCAGATGGGCTCTC	NM_010573
qlrx1_rev	TTCGTTGAGCCAGGCTTTCA	
qPitx2_for	GTGGACCCTCTCGAACTTG	NM_001042504
qPitx2_rev	CTCCATTCCCGGTTATCGGC	
qMyocd_for	GCTGAGACTCACCATGACAC	NM_145136
qMyocd_rev	TGGACCTTTTCAGTGGCGGTA	
qFoxC1_for	CAACATCATGACGTCGCTGC	NM_008592
qFoxC1_rev	CTCTGGCCCGGAGAGTAGG	
qBmp2_for	ATCACGAAGAAGCCGTGGAG	NM_007553
qBmp2_rev	CTCGTCACTGGGGACAGAAC	
qBmpr2_for	AGGTGGCCGAACAATCCA	NM_007561
qBmpr2_rev	TCTTGTGTTGACTCACCTATCTGT	
qFgfr2_for	CACGACCAAGAAGCCAGACT	NM_010207
qFgfr2_rev	CTCGGCCGAACTGTTACCT	
qSmad3_for	AAGAAGCTCAAGAAGACGGGG	NM_016769
qSmad3_rev	CAGTGACCTGGGGATGGTAAT	
qAcvr2a_for	TCCTACTCAAGACCCAGGACC	NM_007396

qAcvr2a_rev	TCTGCCAGGACTGTTTGTCC	
qRyr2_for	GACTGAGGAAGGATCAGGGGA	NM_023868
qRyr2_rev	TTGTTGCCGGTCTGAGTTCT	
qKcnq1_for	ACTTCACCGTCTCCTCATTGT	NM_008434
qKcnq1_rev	AGAGGCGGACCACATATTCTG	
qKcnj2_for	TCTCACTTGCTTCGGCTCAT	NM_008425
qKcnj2_rev	ACTTGTCTGTTGCTGGTACA	
qFgf10_for	TGCGGAGCTACAATCACCTC	NM_00800
qFgf10_rev	GTTATCTCCAGGACACTGTACG	
qFgf8_for	GCTGAGCTGCCTGCTGTT	NM_010205
qFgf8_rev	GAGAGTGTGCTGCGGTTCC	
qHDAC2_for	CCCGTCAGCCCTCTTGTC	NM_008229
qHDAC2_rev	TGCCAATATCACCATCATAGTAGT	
qRai_for	CTTGGTGACAGCAGCGACAG	NM_198409
qRai2_rev	CCACGTGGCCTCGGGAT	
qXrcc4_for	GCAAACCACGGTATTAGCGG	NM_028012
qXrcc4_rev	TGGCTACCTCTCAGTACTCCA	

Primers used for Mef2c isoforms absolute quantification

Primer Name	Sequence 5'→3'
Mef2cTotal_for	ACGAGGATAATGGATGAGCGT
Mef2cTotal_rev	CAGCTTGTTGGTGCTGTTGAA
Mef2cRefSeq_for	GGCAAAGCTTCGGTGTTTCAT
Mef2cRefSeq_rev	CTGCTGAGGGCTTTGTTGTC
AK0077603_for	GGTCAGCCTGTCCAAAAGGA
AK0077603_rev	ACAATGGATGTCAGTTGACCCA

Primers used for ChIP analysis

Primer Name	Sequence 5'→3'
Mef2c-1,5Kb_for	CTGATGGAGAGGTTGGGACT
Mef2c-1,5Kb_rev	ATGCAAGCACCTCTCTCACT
Mef2c-1Kb_for	CTGATGGAGAGGTTGGGACT
Mef2c-1Kb_rev	ATGCAAGCACCTCTCTCACT
Mef2c-200bp_for	GAATGGCAAATAACTACAGTGCT
Mef2c-200bp_rev	TCCTCATTTACACAGGCTT
Mef2c_AHF_for	TCAGTGTCTGCTCCTGCTTC
Mef2c_AHF_rev	TTCCCTCCACACCTTACTGG
Mef2c_-13Kb_for	CTTGCAATTACTACCACTCACA
Mef2c_-13Kb_rev	CCTGTCTCAGTCTGCTCA
Mef2c+2,7Kb_for	GGGGTGGGAATTTAATCA
Mef2c+2,7Kb_rev	GTCTGGTCAATGAGGAGGT
Mef2c_+150Kb_for	TCAAAGAAACTGAGCTACTGTCT
Mef2c_+150Kb_rev	GATGTCACACTAGATCCACAGT
Mef2c_3'UTR_for	CAGTGTCTGTCGTGCGTTTT
Mef2c_3'UTR_rev	ACCCAATTCACACCTTCCCA
Mef2c_-9,6Kb_for	AGTGAAGGAAGAAAAGGTGCA
Mef2c_-9,6Kb_rev	GCTGGCGTTTTGTGTTCTTT
Mef2c_-12Kb_for	ACCCAGAGACACAGGCATAA
Mef2c_-12Kb_rev	TTCCCTTTGCGGTTCCAATG
Mef2c_-14Kb_for	CTCAACTGGTGGTGTAGC
Mef2c_-14Kb_rev	GCTCAACTGGTGGTGTAGC
Mef2c_-6,5Kb_for	TGAGGTCCCATTGTTGATGC
Mef2c_-6,5Kb_rev	TGTCCTCCACAGTTCTTCA
Mef2c_-7,5Kb_for	TGTGTTCCATTACAGCAGAGG
Mef2c_-7,5Kb_rev	CCCCAAGAACATGCATGGT
Hand2_promoter_for	TTACCCACCCCTGTAATC
Hand2_promoter_rev	AATTGCCGAGGTCCTCTTCT
Hand2_OFTRV_for	CTCAGAGCCAGCCAACTACT
Hand2_OFTRV_rev	TCACTCCTCACTGACAGCAC
Actin_for	GGAGCGGACACTGGCACAGC
Actin_rev	ATGCCACACCGCGACCCTA
Intergenic_for	AAACCTCAAAGCCCAGGACACA
Intergenic_rev	ACTTGGTCCCGAGTTGATGGAA

Primers used for 3C-seq Analysis

Mef2cpromoter_F ACACTTGTGCAGAGGGATC

Mef2cpromoter_R AAGCTTTCTAATTTGGGAGC
Mef2cAHF_F TTAATTTTACTACTAACATTGGAGGATC
Mef2cAHF_R AAGCTTGTGCTCTGTGACA

Primers used for 3C-qPCR Analysis

Primer Name	Sequence 5'→3'
3C_Mef2cAHF	TTAATTTTACTACTAACATTGGAGGATC
3C_Mef2c prom	GGGTCACACATCAAGGGTCT
3C_Mef2c-13Kb	CCTTGCCCAGAATGATCAGC
3C_Mef2c+2,7Kb	CCTTTGGCTCTCTCCTATCCT
3C_Mef2c +150	GCAGAGATTAGCCAGTCTATGC
3C_Mef2c 3'UTR	CCAAGCCGCATATCTACTGC
3C_Mef2c Negative	TGCTGACTCAGCTGTGGAG
3C_Mef2c Negative2	ACCCAAGAAATTTTGAGAACCAA
3C_Mef2c Negative3	AACTGCAGCTTGTTTCACGT
3C_Mef2c Negative4	TAGGGGTGGCTTCTGGTTTT
3C_Mef2c Negative5	TGCTTTCCACATTACTGAAGA
3C_Ryr2	CAAATGTAGTGGTGGGTGCC
3C_FoxC1	CAGCCCAAAGATGTTTCAGGT
3C_Bmpr2	TGGATGAGTGGATGGGTAGA
3C_Bmp2	CACACGCCATCACTTAGCAG
3C_Fgf10	AGTGTTAGGATGCAGGGCTT
3C_Acvr2a	ACTCTGAAGGCTGGGAGTTC
3C_Isi1	GCTTAAAGAGGCAGGCTCC
3C_Smad3	AATATGTCCCAAATGTTTCACAGAA
3C_Myocd	CCACCATGGTCACTCTGTCC
3C_Kcnq1	AGGAACCACTCTCCCAAAGG
3C_Kcnj2	ACCGGTTAGCATGGTTTTAGC
3C_Rai2	GAGAGGCTGGAGGGAAGAAA
3C_Xrcc4	GGGTCCATGATTTGCCAAGA
3C_Hand2prom	CGAGCCGGCCCTAAAGATGTA
3C_Hand2 OFTRV_Niall	AAGCTTTAGACCCCTGGATTG
3C_Hand2Negative1_Niall	CTTCCCTGTACATCACCCCT
3C_Hand2Negative2_Niall	GCATTTCCAGCAAGCATCCT
3C_Hand2Negative3_Niall	CTTGTTGGGGTGAGAAGGG
3C_Hand2Negative4_Niall	CACAGGGCAGTTAGGTCTCA
3C_Hand2 OFTRV_Dpnll	TGTTGTTGTTGGTGGTGGTG
3C_Hand2Negative1_Dpnll	CTAAGGGCTTCTGTTGACACC
3C_Hand2Negative2_Dpnll	CCCATAGGCCTTGTCTGGA
3C_Hand2Negative3_Dpnll	CTAAGGTGGCTGGGACTAGG
3C_Hand2Negative4_Dpnll	CGTGTGCTGTGTCTTCTCTT
3C_Actin_F	CTTCTGACCTAGAACTCTTGATCCC
3C_Actin_R	CCCTCTACACACTCAGAATTCATC

SUPPLEMENTAL EXPERIMENTAL PROCEDURES:**Plasmids:**

pcDNA3-IsI1, pcDNA3-IsI1 Δ LIM1, pcDNA3-IsI1 Δ LIM2, pcDNA3-IsI1HOMEO are described elsewhere (Witzel et al. 2012).

Ldb1 and Ldb1 truncated proteins were amplified from mouse cDNA and cloned into the BamHI site of pcDNA3-Flag-HA vector. The following primers were used for amplification:

Ldb1 Ldb1_F 5' gatccatgtcagtgaggctgtgcctgtcc 3'
 Ldb1_R 5' ggatcctcactgggaagcctgtgacgtgg 3'

Ldb1 Δ LID Ldb1_F 5' ggatccatgtcagtgaggctgtgcctgtcc 3'
 Ldb1 Δ LID_R 5' ggatcctcagagagcgaaggctgtggctgggc 3'

DN-Ldb1 DN-Ldb1_F 5' ggatccatggagcccgcacgacagcagcccag 3'
 Ldb1_R 5' ggatcctcactgggaagcctgtgacgtgg 3'

The pCS2+Flag-HA-DN-Ldb1 plasmid was generated by subcloning the Flag-HA-DN-Ldb1 HindIII - EcoRV insert of pcDNA3-Flag-HA-DN-Ldb1 in the blunted BamHI site of pCS2+. Lentiviral constructs were created by subcloning of the Flag-HA-Ldb1 or the Flag-HA-DN-Ldb1 HindIII - EcoRV insert from pcDNA3 plasmids into the blunted BamHI site of pRRL.sin18-IRES-GFP.

Mef2c promoter and AHF enhancer were cloned from wild type mouse (C57BL/6) genomic DNA in pJet1.2 (Fermentas) and subsequently subcloned in pGL4-luciferase plasmid (Promega).

The following primers were used for amplification:

Mef2cpromoter_F 5' gagctctcactgaaagtgatttgac 3'
 Mef2cpromoter_R 5' agatotttctccccacccaagcctct 3'
 Mef2cAHF_F 5' ggatccattaaaatagtactctgca 3'
 Mef2cAHF_R 5' gtcgacgggcccattaacttccaatc 3'

Cell Culture and Transfection

HEK293T, and COS7 cells were grown in DMEM (Invitrogen) supplemented with 10% FBS (Invitrogen), 2mM L-Glutamine, 100U/ml Penicillin and 100 µg/ml Streptomycin (Invitrogen) at 37°C/5%CO₂. Undifferentiated embryonic stem (ES) cells were maintained on mouse embryonic fibroblast (MEFs) feeder cells in DMEM supplemented with 15% fetal bovine serum (FBS, Invitrogen), 2 mM L-Glutamine, 0.1 mM 2-mercaptoethanol (Sigma), 0.1 mM non-essential amino acids (Invitrogen), 1 mM sodium pyruvate (Invitrogen), 4.5 mg/ml D-glucose, and 1,000 U/ml of leukemia inhibitory factor (LIF ESGRO, Millipore). To induce EB formation, dissociated ES cells were cultured in hanging drops of 500 cells per 15 µl of ES cell medium, in the absence of LIF. After 2 days in the hanging drop culture, the resulting EBs were transferred to bacterial culture dishes. For the transfection of HEK293T, cells were seeded at a density of $2 \cdot 10^6$ cells/10cm dish and transfected with 10-20µg DNA using calcium phosphate precipitation. COS7 were transfected using FuGENE® HD Transfection Reagent (Roche), according to the manufacturer instructions. For stable expression, ES cells were transduced with pRRL.Sin18.PGK-GFP-IRES (control construct) and pRRL.Sin18.PGK-GFP-IRES-IsI1, pRRL.Sin18.PGK-GFP-IRES-Ldb1, pRRL.Sin18.PGK-GFP-IRES-DN-Ldb1 or in combinations. Transduced cells were FACS sorted for GFP expression and used for EB differentiation.

Luciferase Assay

For Luciferase Assays, 3×10^4 COS7 cells were seeded in 24 well plates (details in Figure 6). 48h after transfection, cells were lysed in 100 µl lysis buffer (Promega, Luciferase Assay System) and luciferase activity was measured on Mirthras LB 940 (Berthold Technologies) according to the Luciferase Assay System Manual (Promega). β-galactosidase assays were performed using CPRG as substrate (Sigma).

RNA Isolation

RNA was isolated using the TRIzol Reagent (Invitrogen). cDNA was synthesized with the High-Capacity cDNA Reverse Transcription Kit (Applied Biosystems), and real-time PCR was

performed using the SYBR Green PCR Master Mix (Applied Biosystems). The cycle numbers were normalized to GAPDH (ES/EBs and Embryos). Primer pairs are described in Table S2.

Immunofluorescence of Embryoid Bodies (EBs)

EBs were collected, washed with PBS, embedded in 17% gelatin and fixed O/N at room temperature in 4% PFA. Next day the EBs were sectioned with vibratome at 70 μ m. The obtained sections were fixed in 2% formaldehyde, 0.1M PIPES, 1.0 mM MgSO₄, 2.0 mM EGTA O/N at 4°C, followed by 1 hour blocking (4% BSA + 0.4% Triton X-100) and incubated with primary and secondary antibodies diluted in blocking solution.

Flow Cytometry

For FACS analysis the EBs were dissociated, 1×10^6 cells were washed with 1 ml PBS and blocked in 100 μ l FACS buffer (10% FCS in PBS) for 1 hour at room temperature. After blocking, the cells were stained with 0.5 μ g each APC-conjugated anti-Flk1 (e-Bioscience 17-5821-81) and PE-conjugated anti-PDGFR α (e-Bioscience 12-1401-81) or control rat IgG2a K isotype APC- (e-Bioscience 17-4321) or PE-conjugated (e-Bioscience 12-4321) antibodies. After PBS washes, cells were fixed for 10 minutes at room temperature in 2% PFA. Data were acquired on an LSRII flow cytometer (BD) and analyzed using FlowJo software.

Chromatin immunoprecipitation

Embryoid bodies at day 4 or 5 of differentiation were dissociated with trypsin to obtain single cells suspension and resuspended with complete differentiation medium to obtain a concentration of 10^6 cells/ml. Cardiogenic region of 30 E8-9 embryos was dissociated with trypsin to obtain single cells, and resuspended in PBS containing 10% FCS. For chromatin immunoprecipitation 0.5 to 1×10^7 cells were fixed with 1% formaldehyde for 10 min. Formaldehyde was quenched with glycine at a final concentration of 125 mM and washed three times with PBS. Cells were lysed in L1 lysis buffer (50 mM Tris pH8, 2 mM EDTA pH8, 0.1% NP-40, 10% glycerol) for 5 min, the nuclei were spun down and resuspended in L2 nuclear resuspension buffer (1% SDS, 5 mM EDTA pH8, 50 mM Tris pH8), followed by sonication to

fragment the chromatin. The samples were centrifuged, diluted 1:10 with DB-dilution buffer (0.5% NP-40, 200 mM NaCl, 5 mM EDTA, 50 mM Tris pH8) and incubated with primary antibody overnight at 4°C, followed by 3 h incubation with Protein-A/G Sepharose beads (GE Healthcare). Immunoprecipitates were washed two times with NaCl-washing buffer (0.1% SDS, NP-40 1%, 2 mM EDTA, 500 mM NaCl, 20 mM Tris pH8), followed by two washes with LiCl-washing buffer (0.1% SDS, 1% NP-40, 2 mM EDTA, 500 mM LiCl, 20mM Tris pH8) and eluted with EB-extraction buffer (TE pH8, 2% SDS). Cross-linking was reverted by overnight incubation at 65°C, DNA was purified and subjected to qPCR analysis. Primer pairs are described in Table S2.

GO Analysis

GO analysis was performed using DAVID software (Huang da et al., 2009a, b).

Histological analysis

Embryos were dissected in ice cold PBS, fixed in 4%PFA O/N at 4°C, dehydrated in Ethanol and stored at -20°C. For histological analysis, the tissues were incubated in 100% xylol and embedded in paraffin for further processing. Embedded organs were sectioned using an RM2245 microtome (Leica) and Hematoxylin-Eosin (H&E) staining was performed.

REFERENCES:

- Huang da, W., Sherman, B.T., and Lempicki, R.A. (2009a). Bioinformatics enrichment tools: paths toward the comprehensive functional analysis of large gene lists. *Nucleic acids research* 37, 1-13.
- Huang da, W., Sherman, B.T., and Lempicki, R.A. (2009b). Systematic and integrative analysis of large gene lists using DAVID bioinformatics resources. *Nature protocols* 4, 44-57.